INTEGRATED FIELDWORK 2024

ZAININGEN

Geodäsie und Geoinformatik
Geomatics Engineering
University of Stuttgart

0.1 List of students and supervisors

0.1.1 Students

- Rebecca Kölbel
- Jos Vaihinger
- Niels Stahl
- Yash Bankar
- Hussein Salman
- Mehdi Mohammad Baba
- Soheil Ettehadieh

0.1.2 Supervisors

- Institute of Engineering Geodesy (IIGS)
  - Ronja Miehling (M. Sc.)
  - Dr.-Ing. Gabriel Kerekes
  - Pauline Speidel as assistant
- Institute of Geodesy (GIS)
  - Ron Schlesinger (Dipl.-Ing. (FH))
- Institute of Photogrammetry (IfP)
  - Dr.-Ing. Michael Cramer
  - David Collmar (M. Sc.)
  - Dr. Lida Asgharian Pournodrati
- Institute of Navigation (INS)
  - Clemens Sonnleitner (M. Sc.)
  - Vanessa Bär (M. Eng.)

Contents

1

Introduction

Baden-Württemberg was significantly influenced by the Celts, an ancient European people known for their rich culture, advanced metalworking skills, and complex social structures. The Celts inhabited this area from the late Bronze Age through the Iron Age, leaving a profound legacy that can still be seen in numerous archaeological sites across the region. They are characterized by significant advancements in metalworking, trade, and societal organization.
One of those practices was burial practices, often by burying their dead in large mounds or tumuli. The mounds were used to bury prominent individuals, likely those of high status such as chieftains or warriors. Additionally, building burial mounds was a way to maintain and pass down cultural traditions. It reflected shared values and practices within Celtic society, ensuring continuity across generations. The construction of burial mounds could also serve to mark territory and assert control over a particular area. These mounds were visible indicators of the community's presence and its claim to the land. These burial sites contain valuable grave goods that provide insights into their beliefs, social hierarchy, and way of life.

One burial mound was found in Zainingen, a village part of the community Römerstein on the Swabian Alb. The area of interest is located 1.5 km northeast of Zainingen in the "Au" field between the crossing of B28 from Bad Urach to Blaubeuren and B456 to Kirchheim unter Teck.
The Zainingen burial mound field is a significant archaeological site in Baden-Württemberg, offering valuable insights into the burial practices and societal structures of the Celtic civilization during the Hallstatt period. This cemetery is one of the largest and best-preserved monuments of the Hallstatt culture in the region, featuring 62 mounds that date from the 9th/8th century BC to the 6th/5th century BC.

Figure 1.1: *Measurement area (from Google Maps)*

Modern surveying methods, including 3D terrain acquisition, laser scans, and classical surveys, are crucial for documenting and preserving this heritage site.
By studying these burial mounds, 3D documentation was constructed to include aspects of Celtic life, offering a glimpse into their world and enhancing the knowledge of European prehistory. The preservation and documentation are passing a long process on 6 different tasks performed in this project.

The first task includes creating a 3D network via static measurements with GNSS antennas. At first build up eight GNSS antennas over eight known trigonometric points. The antennas should measure at the same time and one hour. After post-processing there are got coordinates with accuracy of few centimetres. Two of the points are located in the area of burial mounds near Zainingen, the area of interest. These points are unknown. So with the GNSS measurements the points become to known points and they can be used as reference points for the following tasks.

The second task is about creating a 3D network via robotic total station. The two GNSS points are used for the transformation from local coordinates calculated by the measurements in the field into a global coordinate system. Also they are used as reference points to expand to a network which envelops the entire area. Seven more points are created. Later, all reference points are used for free stationing, so they should be well distributed over the entire area so that free stationing is possible on every location.

In the third task the area is measured by height transfers via geometric levelling. There are defined two long loops which start at the same benchmark with known height. The ends of the loops are the GNSS points from task 1. The loops pass also some of the reference points of task 2. In the loops are defined standing points for staffs and the digital level. The height differences between the standing points of the instrument are measured. With these differences the heights of the reference points can be calculated

and added to 3D network.

In task 4 one drone (DJI Phantom 4 RTK) flies over the area of interest to take images which are used to create a surface model and to calculate the Normalized Difference Vegetation Index (NDVI).

Task 5 is about terrestrial laserscanning. From different standing points the whole area is measured by laser scanner. The received point clouds are used to create a surface model. In the point clouds three to four black& white-targets should be located. With these the different point clouds can be merged to one of the whole area.
Because of every surveying measurement has to have a georeferencing the black & white targets will be measured by a total station stationed between known reference points of task 2.

In Task 6 a RTK Rover is used to acquire GNSS data for comparison with other tasks. The measurements can be performed in static, kinematic and automatic (kinematic) mode using predefined routes. Post-processing allows different methods of evaluation and study different scenarios.

At the following pages the plan, performance and results of every task are described detailed.

2

Tasks

2.1 3D Network via GNSS

Introduction

In the region of Celtic mounds and Roman forts, a reference network is established between known State survey points in order to set up new points in area of interest in both Zainingen and Donnstetten. The survey employes the static GNSS survey technique, involving multiple 1-hour data collection sessions with 8 GNSS receivers. Leica Infinity is used to process the observation for a 3D network in the global WGS84 coordinate system.

Planning phase

1. Selection of points
   We identified 8 useful state survey points from the available options, ensuring they were strategically located and reliable for our task.
2. Addition of new points
   4 new points (Z1,Z2,D1,D2) in both locations are added to our survey and to the accurately determinition of the coordinates, enhancing the coverage and precision.
3. Session planning
   Each selected point is measured four times, with each session lasting at least one hour. This ensures thorough data collection and redundancy.
   Considerations in planning several critical factors are considered:
   - Distance and Travel Time: Efficient routes are planned to minimize travel and setup time.
   - PDOP: Measurement sessions are scheduled to avoid high Positional Dilution of Precision periods, ensuring data accuracy.
   - Equipment Constraints: With only 8 GNSS receivers, careful coordination ensured all points are measured adequately and switching the receivers.
   - Time management: Planning enough time for setting up and repositioning in between the sessions, therefore also planning the repositioning of the

receivers to the closest point.

SESSION PLAN TASK 1 - INTEGRATED FIELDWORK 2024												
SCHEDULE			RECEIVER & LOCATIONS							
DAY ↓	TIME (CEST) ↓	SESSION ↓	1	2	3	4	5	6	7	8
MONDAY 15.07.2024	12:00-13:00	S1	D1	D2	Z1	Z2	141	34	80	86
	14:20-15:20	S2	84	86	147	141	Z1	Z2	D2	D1
TUESDAY 16.07.2024	10:20-11:20	S3	Z1	34	D1	D2	84	80	147	Z1
	12:10-13:10	S4	141	147	80	84	D1	86	34	Z2
WEDNESDAY 17.07.2024	10:30-11:30	S5	80	84	86	D2	34	141	Z2	147
Transported by:			CAR 1		CAR 2		CAR 3		CAR 4	

Figure 2.1: *Session plan*

Field Work

Task 1 was performed in the first three days, with an introduction for everyone on the first day to ensure the data is collected and processed until Wednesday evening. During the fieldwork, expected complications were encountered, such as inexperience with the devices or issues with the devices themselves as well as misplaced devices during the first session which let to changes in the schedule during the measurements, however this had no influence on the overall schedule and the task could be finished in time.
The collected GNSS data was processed using the Leica Infinity software, following these steps:

- Importing the raw GNSS data into the software
- Trimming the data to ensure we have a good overlap.
- Processing the data to obtain preliminary coordinates
- Adjusting the network to refine the coordinates
- Analyzing the precision and accuracy of the results

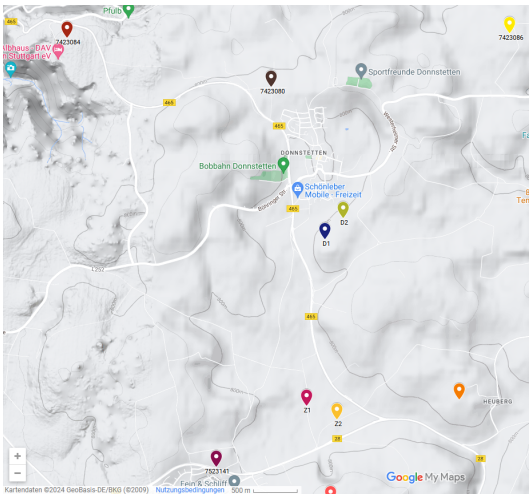

Figure 2.2: *Map overview [1]*

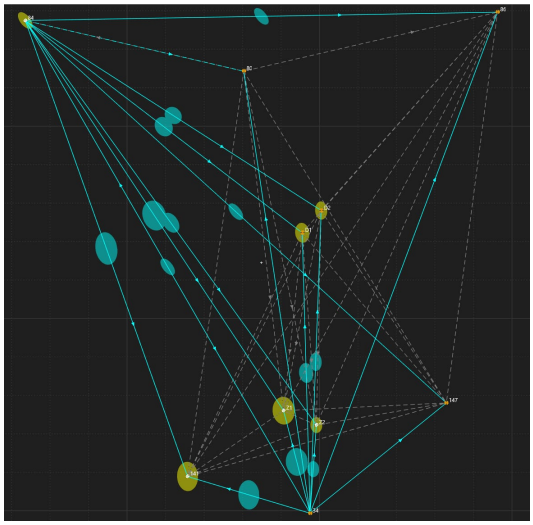

Figure 2.3: *Network in Infinity*

Evaluation and Results

The following table represents the final results of task 1, containing all State points and new points of both locations.

Table 2.1: *Task 1 results all points*

Point ID	Easting(m)	Northing(m)	Height(m)	Std(E) [m]	Std(N) [m]	Std(H) [m]
Z2	32541967.188	5370892.006	779.403	0.003	0.004	0.008
Z1	32541626.540	5371041.210	777.596	0.005	0.007	0.014
D2	32542017.434	5373122.991	835.940	0.003	0.004	0.003
D1	32541820.510	5372891.011	813.110	0.003	0.004	0.003
147	32543318.150	5371121.740	832.478	0.000	0.000	0.010
141	32540628.712	5370357.031	814.671	0.005	0.007	0.014
86	32543849.530	5375185.330	839.873	0.000	0.000	0.010
84	32538941.821	5375099.300	781.666	0.002	0.003	0.006
80	32541212.180	5374571.600	819.568	0.000	0.000	0.029
34	32541902.260	5369974.390	862.523	0.000	0.000	0.005

The analysis of the results indicates the following points regarding the accuracy and precision of the measurements:

- Standard Deviations: The small values of standard deviations (0.000 - 0.005 m for Easting and Northing, and around 0.003 - 0.029 m for height) indicate high precision in the measurements
- Consistency Across Measurements: The consistency in standard deviation values across different points suggests reliable data collection and processing

Table 2.2: *New Points: GNSS and SAPOS difference*

Point		East [m]	North [m]	Height [m]
Z1	GNSS	32541626.540	5371041.210	777.596
	SAPOS	32541626.545	5371041.204	777.722
	Δ(SAPOS,GNSS)	0.005	0.006	0.126
Z2	GNSS	32541967.188	5370892.006	779.403
	SAPOS	32541967.198	5370892.025	779.549
	Δ(SAPOS,GNSS)	0.0100	0.019	0.146
D1	GNSS	32541820.510	5372891.011	813.110
	SAPOS	32541820.522	5372890.995	813.236
	Δ(SAPOS,GNSS)	0.0120	0.016	0.126
D2	GNSS	32542017.434	5373122.991	835.940
	SAPOS	32542017.435	5373122.973	836.094
	Δ(SAPOS,GNSS)	0.0010	0.018	0.154

Analysis of GNSS and SAPOS Coordinate Differences The objective of this analysis is to compare the differences between GNSS and SAPOS coordinates across several

survey points. The data consists of differences in Easting, Northing, and Height for four points: Z2, Z1, D2, and D1. The aim is to assess the precision and accuracy of GNSS measurements in comparison to SAPOS.

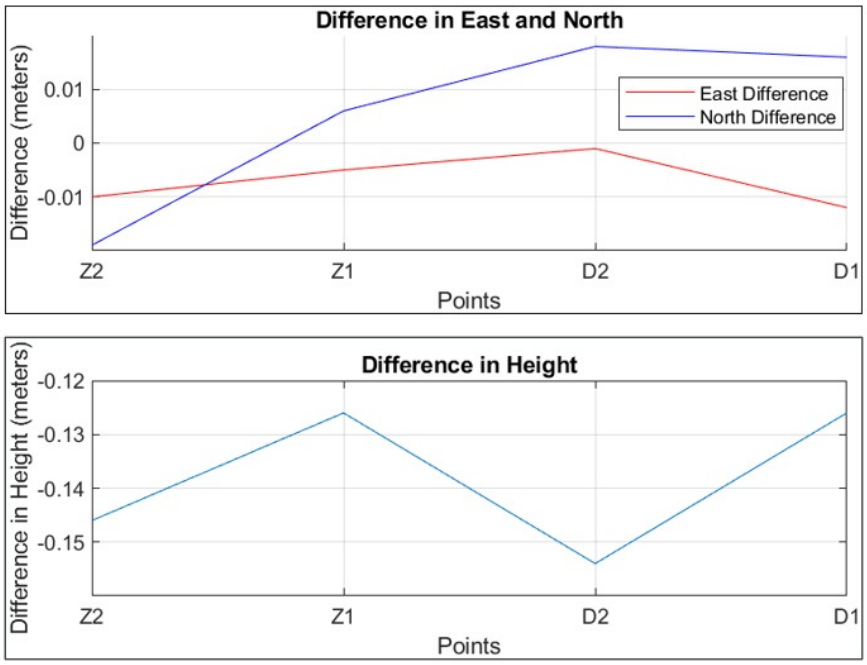

Figure 2.4: *Visualized differences GNSS/SAPOS*

The plot indicates the following:

1. Easting Differences: The differences in the Easting coordinates range from 0.001 m (D2) to 0.012 m (D1), showing minimal variation among the points.
2. Northing Differences: The Northing differences vary slightly more, ranging from 0.006 m (Z1) to 0.019 m (Z2).
3. Height Differences: The Height differences range from 0.1260 meters (Z1 and D1) to 0.154 m (D2).

Interpretation

The analysis reveals that the differences between GNSS and SAPOS coordinates are generally small, indicating good agreement between the two measurement systems. However, some variation exists, particularly in the Height component. This variation could be attributed to several factors, such as:

- Measurement Precision: Differences in the precision of the instruments used for GNSS and SAPOS measurements.
- Environmental Factors: Variations in environmental conditions during the measurements, such as atmospheric conditions, multipath effects, and satellite geometry.

- Systematic Errors: Potential systematic errors inherent in one or both measurement systems.

It is also important to note, that the State provided data dates back to 1981, where GPS measurements where lacking precision, as well as the fact that the markings of the points, e.g. 141,

Figure 2.5: *Image showing point 141 marking*

are often in a bad condition and the exact center is not visually recognisable.

Conclusion

Overall, the GNSS system demonstrates a high level of accuracy and precision, closely matching the SAPOS reference system.

The GNSS survey successfully delivered high-precision coordinates for the surveyed points. The analysis confirmed the reliability and accuracy of the measurements, with minimal differences between GNSS and SAPOS coordinates. The low standard deviations observed indicate that the survey results exhibit high precision and minimal error. These results are well-suited for applications requiring high accuracy, such as geodetic control and detailed engineering surveys.

RESOURCES

1. Google My Maps State point and new point project:
   https://www.google.com/maps/d/u/0/
   edit?mid=1ydF_RGKZWgv3j7j0u7wvcbsDwgY_E_k&usp=sharing

2.2 3D Network via total station

Introduction

The goal of task 2 is to create a stable, precise and high redundant 3D geodetic network via robotic total station surveying. Total stations are used because of their detailed measurements and precise stakeouts.
Therefore, reference points are created which are distributed over the entire area of measurement. It is important to measure different configurations with free lines-of-sight to reach the requirements.

Planning phase

The robotic total station Trimble S7 is used.
In addition to the GNSS points of task 1, seven more reference points are planned. To catch every of the nine points at least three times from different standing points, six to seven standing points of total station are needed. From each standing point it is possible to measure five reference points. They are always measured in two faces and five rounds to get enough measurement values and to do an accurate adjustment.

Figure 2.6: *Planned standing points and reference points*

Field Work

At first the total station Trimble S7 has to be built up on a tripod. The instrument has to be levelled.
The whole control is working with a controller. After creating a new job and entering the temperature and air pressure, give a name for the standing point. Then the prism height is entered in the controller.
After that, the measurement can start. If every prism is sighted out, the automatically

measurement can start to measure the second face and then in total five rounds.
When it is finished the total station can move to the next standing point and the prisms are built up on the next used reference points.

Figure 2.7: *Robotic total station Trimble S7*

Figure 2.8: *Prism built up on reference point*

Evaluation and Results

The measured values are imported into the software JAG 3D as column-based data. For the adjustment, several inputs are needed: the names of the standing points, names of aiming points (here: reference points), horizontal angles, vertical angles, slope distances, and target heights. The two GNSS points are defined as datum points. With this data it is possible to calculate the first adjustment.
The goal of adjustment is to get a realistic but precise enough result with accurate coordinates of the reference points. Therefore a general standard deviation of about 1 mm and an accuracy of every coordinate of all reference points in area of sub-millimetres should be reached. For every adjustment, the Gauss-Markov-model is used .
In the first version of adjustment, the worst measured values are detected as gross errors via a function in JAG 3D called ”probability of exceeding”. The limits are set as $0 < 2.0 < 3.0 < 100$ which are the recommended settings to find gross errors. The values, which are detected, can be eliminated now. This is possible to do because of a high redundancy about 90 %.
During trying to eliminate all imprecise measurements, it is outstanding that all vertical angles measured from standing point S7 are inaccurate. So the whole standing point is eliminated and the adjustment done again. The general standard deviation improves from around 80 mm to 7 mm. After eliminating some more gross errors the general standard deviation has a value of 2.25 mm. All coordinates have an accuracy of about 0.4 mm to 0.9 mm in x- and y-direction and 0.8 mm to 1.3 mm in z direction. In the following tables, the detailed accuracies of every reference point can be seen.

	$\sigma_y[mm]$	$\sigma_x[mm]$	$\sigma_z[mm]$
Z1	0.3	0.4	0.8
Z2	0.3	0.3	0.8
T1	0.3	0.3	0.6
T2	0.3	0.4	0.6
T3	0.4	0.5	1.0
T4	0.5	0.5	1.0
T5	0.3	0.4	0.6
T6	0.3	0.3	0.6
T7	0.6	0.4	1.3

Table 2.3: *Accuracies of reference points*

In the plot of the adjusted network (2.9), it can be seen that the accuracies of T3, T4 and T7 are worse than the others because their error ellipses are bigger than the ellipses of the other points. The reason is that they are situated at the border of the area. They are measured only from approximately one direction. But be careful with the size of the error ellipses; here the scale is 1000:1, so they are shown bigger than they are in reality.

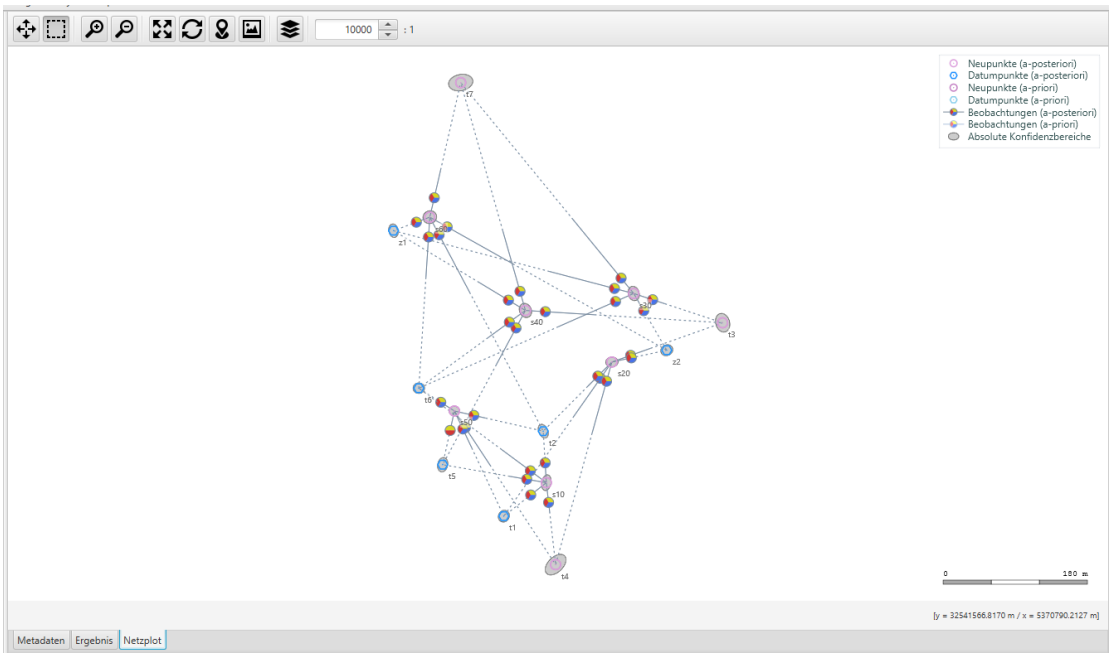

Figure 2.9: *Plot of adjusted network*

Another try of the adjustment is done to reach a better accuracy. A "Baarda test" detects the worst measurements. After eliminating all imprecise measured values, the general standard deviation is around 8 mm and the standard deviations of the coordinates are around 0.4 mm to 2.0 mm. There is no improvement in comparison to the adjustment done before, so the first adjustment is used for the following steps.
To transform the local network/coordinates into global UTM coordinate system (Uni-

versal Transverse Mercator), the UTM-coordinates from GNSS measurements (task 1) for Z1 and Z2 and the heights of the reference points measured by levelling (task 3) are entered. The adjustment calculates the global UTM coordinates for the other reference points. The accuracy is the same after the transformation as before.
While comparing the adjusted coordinates of Z1 and Z2 with the coordinates from GNSS measurements, a variation for Z1 in y-direction about 11.13 cm and in x-direction about 6.76 cm and for Z2 in y-direction about 3.13 cm and in x-direction about 11.08 cm is noticeable.

There could be possible reasons for the variation to GNSS coordinates:

- inaccurate vertical angles in general
- measured prism heights are not precise enough
- distribution of standing points improvable → reference points are sighted out from approximately same direction
- measured height of wooden peg on T2 and T3 inaccurate
- difficult to level the prisms on T2 and T3 because of the wooden peg
- too many measurements eliminated in the adjustment, so the network is fixed too much
- reference points can be only marked on the tracks because of mowing work, better distribution is not possible
- GNSS accuracy about 1-3 cm

For checking the network and looking for the fault, various measurements are done: All reference points are measured with RTK measurements.
To check the inner geometry of the measured and adjusted network, the horizontal distance between Z1 and Z2 is measured with total station.
This distance is compared with the distance calculated from the GNSS coordinates, with the distance calculated from RTK coordinates and with the distance calculated from the adjusted coordinates.

Distances:

$$s_{GNSS} = \sqrt{(626.540 - 967.188)^2 + (1041.210 - 892.006)^2 + (777.596 - 779.403)^2} = 371.8954 \text{ m} \quad (2.1)$$

$$s_{RTK} = \sqrt{(626.653 - 967.2988)^2 + (1041.251 - 892.0373)^2 + (777.779 - 779.5362)^2} = 371.8970 \text{ m} \quad (2.2)$$

$$s_{adj} = \sqrt{(626.4724 - 967.2988)^2 + (1041.3214 - 892.0373)^2 + (777.719 - 779.5362)^2} = 372.0910 \text{ m} \quad (2.3)$$

$$s_{measured} = 372.0764 \text{ m} \quad (2.4)$$

Differences between the calculated distances:

$$\Delta s_{GNSS,adj} = 0.1956 \text{ m} \tag{2.5}$$

$$\Delta s_{GNSS,measured} = 0.1810 \text{ m} \tag{2.6}$$

$$\Delta s_{GNSS,RTK} = 0.0016 \text{ m} \tag{2.7}$$

$$\Delta s_{measured,adj} = 0.0146 \text{ m} \tag{2.8}$$

$$\Delta s_{measured,RTK} = 0.1794 \text{ m} \tag{2.9}$$

$$\Delta s_{adj,RTK} = 0.1940 \text{ m} \tag{2.10}$$

The measured distance matches with the distance calculated with the adjusted coordinates. The difference is about 1.5 cm.
The ”GNSS distance” matches with the ”RTK distance” (variation is about 1.5 mm), but both don’t match with the distance calculated with the adjusted coordinates or the measured distance.

For checking the network and continuing with the other tasks because of time problems, a free stationing is executed. The standard deviation of the coordinates calculated by total station from free stationing are about 12 metres. Looking at the detailed results, it is remarkable that the differences between the measured coordinates for T1 and the imported ones are about 14 metres in y-direction and 3 metres in x-direction.
To get more stable on the results, the free stationing is repeated. The observations are verified, so T1 is never used again for free stationing. For adding it to the network anyway, T1 is measured as new point.
The next free stationings without using T1 have an accuracy of about 4 mm to 1 cm.
As final version of the coordinates, this version of ”detecting gross errors” is used for importing the coordinates into the total station and use them for free stationing for the following tasks because the network itself is accurate enough (2.9).

Unfortunately, during the post-processing at the university one week after the measurements a fault in T1 was detected: the y coordinate has transposed digits in the text file. The error occurred during copying the coordinates from the adjustment into a text file to import them into the total station. But the adjustment is not influenced by this fault and the possible reasons for the offset to GNSS coordinates as mentioned before are still valid.
Because of not using T1 for free stationing, there is also no subsequent fault for the following tasks.

2.3 Height transfer via geometric levelling

Introduction

Usually, the height component can be easily obtained by different methods (GNSS, Photogrammetry, etc.) because of that nowadays it does not get much attention. However, the before mentioned methods usually ignore the fact that they do not provide reliable physical heights, meaning that the height component cannot be used for applications that require high accuracies and physical requirements.
The solution is geometric levelling.

Levelling is basically conducted with a levelling instrument and two vertically posted levelling staffs. Height differences are determined using horizontal lines of sight between points. The levelled height difference between the staffs is given by the differences between the backsight and foresight reading. Modern levelling instruments provide digital results and the achievable accuracy level has reached the sub-mm domain.

The points of the Baden-Württemberg state network used for creating the network in task 1 and task 2 with GNSS and TS are only given as 2D coordinates. In order to get the height for this network we use geometric levelling to transfer the height from a benchmark to the network points.

Planning phase

Primarily a Leica DNA03 is used and for one section a Trimble DINI.

Figure 2.10: *Leica DNA03*

Figure 2.11: *Trimble DINI*

To prepare for the levelling it is necessary to know which height benchmark can be used, for the Celtic burial mound field in Zainingen it is necessary to use benchmark 254 close to the village.

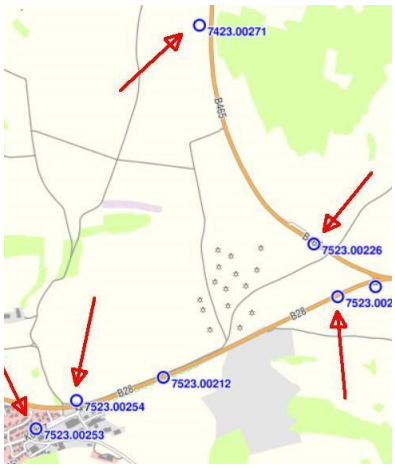

Figure 2.12: *Benchmark Map*

Figure 2.13: *Benchmark 254*

To reach the area of interest and to get the height of the network points (GNSS points, Network points), the levelling line is pulled over a country road.

Field Work

The horizontal line between a staff and the position of the instrument is usually <30m. The distances from instrument position to the two points should be approximately the same in order to eliminate systematic influences from the atmosphere and remaining finish line skew. To meet these requirements, the distances are measured with a tape measure and marked with a paint spray.

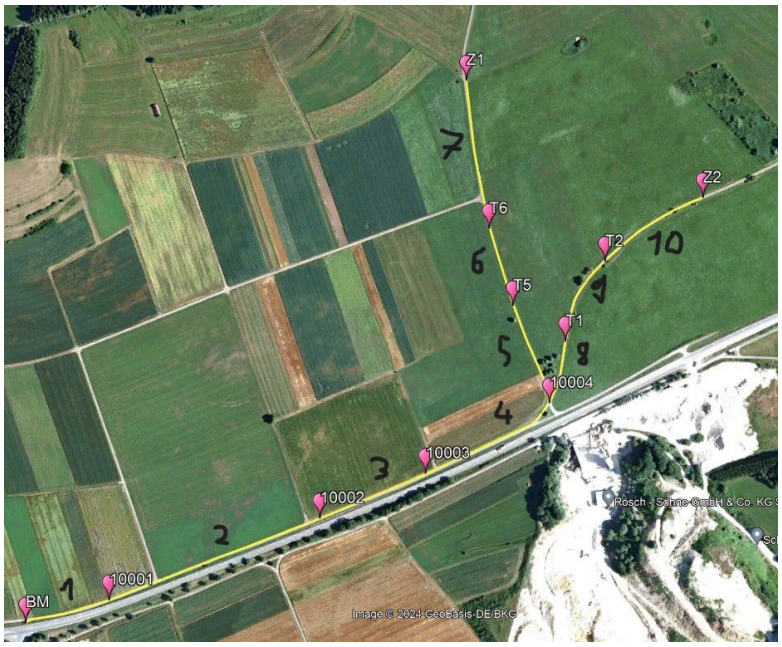

Figure 2.14: *Levelling Lines*

During the area inspection, nails are placed at suitable points to divide the route into smaller sections. Shorter distances enable earlier control of the loop closure error and due to the time-consuming measurement it is an advantage in order to stay focused. The nails and wooden stakes in the target area, which define the sections of the line leveling are used as network points in task 2.

The Näbauer method is used to adjust the instrument. The levelling is carried out using the BFFB method.
To save time, the Trimble DINI is used for section 10 after it is no longer required in the target area in Donnstetten.

Evaluation and Results

Various problems arose during the measurements, such as the previously marked line points needed to be adapted to better suit local conditions. Due to an internal error with the Leica DNA03, which has counted the point numbers on one of the sections incorrectly and due to the use of different instruments, it was necessary to bring the measurements together in one document by hand. When merging, the point numbers are customized to the wanted ones.

Table 2.4: *Task 3 closing error*

Line ID	Lenght [m] (single)	Closing Error [mm]
1	115.39	-0.1
2	300.98	0.7
3	151.19	0.2
4	200.39	0.4
5	155.40	0.2
6	99.99	-0.1
7	199.46	0.5
8	84.39	0.2
9	120.41	0.4
10	186.25	0.06

The loop closure errors are usually within the expected accuracy range. In cases where the error is higher than 1 mm/km, the measurement will not be carried out again because the deviation is not too large.
One of the measurements had to be repeated because the error was to big.

To determine the coordinates of the network points, the location coordinates determined with GNSS (Task 1), the total station measurements (Task 2) and the leveling measurements are combined in one adjustment.

The free program "Jag3D" is used to adjust the network.

Table 2.5: *Task 3 Heights*

Point ID	Height diff. to BM [m]	Height[m]	Adjusted Height [m] | Δ[mm]
BM	-	801.935	-
10001	-2.8742	799.0608	-
10002	-7.7251	794.2099	-
10003	-13.1021	788.8329	-
10004	-15.9214	786.0136	-
T1	-18.8333	783.1017	783.1017 | +0
T2	-20.9982	780.9368	780.9337 | -3.1
T5	-20.9263	781.0087	781.0088 | +0.1
T6	-22.6829	779.2521	779.2504 | -1.7
Z1	-24.2195	777.7155	777.7191 | +3.6
Z2	-22.39984	779.53516	779.5362 | +1.04

By hybrid network adjustment with additional measurements from Task 2, the heights changed a bit, this change is in a domain where bigger errors in levelling can be ruled out.
Since the prisms, in Task 2, are placed in a recess in the nails and the actual prism rod heights cannot be read exactly, there are slight changes in the height due to the adjustment.

To control the measured coordinates of the network points there is a GNSS measurement with SAPOS.

Table 2.6: *Task 3 Heights with SAPOS*

Point ID	Height [m]	SAPOS Height [m] | Δ[mm]
10004	786.0136	786.046 | +32.4
T1	783.1017	783.109 | +7.3
T2	780.9368	780.948 | +11.2
T5	781.0087	781.006 | -2.7
T6	779.2521	779.244 | -8.1
Z1	777.7155	777.722 | +6.5
Z2	779.53516	779.549 | +13.84

Table 3 shows that the height differences between levelling data and SAPOS are in the expected range of few centimeters.

Issues not previously mentioned:
- A long time needed for measurements with Leica DNA03

- The leveling staff wobbled, especially in strong winds
- The instrument (Leica DNA03) vibrated in strong winds

In conclusion the provided heights of levelling are reliable and can be used for the network.

2.4 Airborne data acquisition - photogrammetrical 3D documentation of heritage sites

Introduction

The use of airborne systems for photogrammetric 3D documentation has changed how heritage sites is mapped and preserved. UAVs, or drones, are now the preferred choice for capturing accurate data over small areas, replacing traditional small planes. This method is cost-effective and time-efficient, making it common in fields like agriculture, construction, cultural heritage exploration, and infrastructure inspection. UAVs with advanced cameras can safely reach and document areas that are hard or dangerous for people to access.

In this task, the objective is to generate highly accurate digital surface and terrain models (DSM/DTM) along with orthophotomosaics for Zainingen site. These outputs are critical for documenting and understanding the historical significance and extent of this site. A DJI Phantom 4 RTK drone equipped with a DJI Zenmuse FC6310R RGB camera and a Parrot Sequoia multi-spectral camera are employed. The RGB camera captures high-resolution images for detailed mapping, while the multi-spectral camera captures data in different parts of the electromagnetic spectrum, such as the Red Edge and Near Infrared (735-790 nm). This allows us to create Normalized Difference Vegetation Index (NDVI) maps, which can reveal hidden historical structures based on vegetation patterns.

Planning phase

Methodology:
Flight planning: The target area, a field in Zainingen, requires specific flight plans to achieve the desired ground sampling distance (GSD) and overlap ratios. For the RGB camera, flights are planned to achieve a GSD of 2 cm. These flights have an overlap ratio of 80% front overlap and 60% side overlap, with a maximum altitude of 80 meters.
For the Sequoia multi-spectral camera, a GSD of 5 cm is adequate. The flights for this camera have an overlap ratio of 80% front overlap and 30% side overlap due to its smaller sensor format.

Figure 2.15: *Camera system carried by airborne platform and multispectral Sequoia camera*

Ground Control Points (GCPs): Before starting the flights, mark signalized control points and provide their precise coordinates in the target coordinate system, likely ETRS89 / UTM coordinates with heights above the ellipsoid. These ground control points (GCPs), along with RTK positions acquired by the drone, ensure accurate georeferencing of the final products.
Data acquisition: Ensure all necessary equipment is prepared and a detailed flight plan is created. During the flights, check for unforeseen obstacles and adjust the flight path if necessary. Mark and measure ground control points (GCPs) accurately using terrestrial survey methods.
Data processing: After the flights, process the RGB and multi-spectral images using Agisoft Metashape to create 3D point clouds, orthophotos, DSMs, and DTMs. Additionally, generate false-color composites and NDVI maps from the multi-spectral data to reveal any hidden structures.
Validation: Perform a post-processing analysis to validate the acquired data. Evaluate the accuracy of the georeferencing and final outputs by comparing them with results from automated surface mapping.

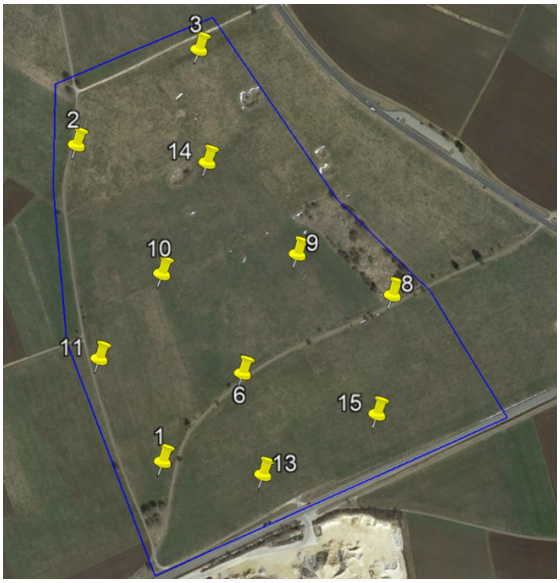

Figure 2.16: *Area of interest in Zainingen*

We prepared all necessary equipment and created a packing list. We visualized and analyzed the area of interest to ensure effective planning and execution of the fieldwork. We planned the number and distribution of signalized control points. We developed a detailed flight plan, including appropriate parameters and justifications for the planned operations.

Figure 2.17: *Flight plan in Zainingen*

Field Work

We checked the area for any unexpected obstacles. We set up the ground control points and marked on-site and, on a sketch, using 11 checkerboards with wooden poles in the designated area. The drone flies for approximately 1 hour to collect data with both cameras. We measured accurately all marked points using ground survey methods. We performed an initial check of the data to ensure its accuracy.
Difficulties and problems during using drone - weather conditions and equipment challenges: Harsh weather conditions, such as wind, rain, and snow, can affect the quality of the collected data. Additionally, battery life may decrease in different weather conditions, which can be problematic during data collection. Therefore, batteries may need to be changed multiple times. Weather conditions can also impact the radiometry of both RGB and multi-spectral images.

Evaluation and Results

Image Processing and Assessment: Process the imagery in Metashape to derive 3D point clouds, orthophotos, DSMs, and DTMs. Generate NDVI maps from the combined RGB and multi-spectral data. Assess the accuracy of the georeferencing and the quality of the final products.
Difficulties with data during during post processing - Time constraints and height system considerations: There is limited time for post-processing after integrating the field data, as it involves many steps and requires powerful GPUs. Also, be aware of differences in height systems, such as ellipsoid and geoid variations.
Steps which are done in Metashape:

1. Cleaning useless photos: Initially, unnecessary photos captured by the Sequoia camera are removed to streamline the processing workflow and optimize storage usage.
2. Aligning photos: Photos from both cameras are aligned into a single chunk, with the exception of the RGB images from the multispectral camera. This step ensured that the images are correctly positioned relative to each other for subsequent processing stages.
3. Adding RTK coordinates: The RTK coordinates are added to 11 control points to enhance the spatial accuracy of the photogrammetric model.
4. Measuring control points: Control points are measured manually due to the impossibility of automating this process. Manual measurement ensures precision in the georeferencing of the images.
5. Cleaning Tie Points: Tie points are cleaned to minimize the reprojection error, improving the overall accuracy and reliability of the photogrammetric reconstruction.
6. Dense Image Matching: A dense image matching process is conducted to generate a detailed and high-resolution point cloud from the aligned photos.

7. Creating Dense Point Cloud: A dense point cloud is created, providing a 3D representation of the surveyed area with a high level of detail.
8. Creating DSM: A Digital Surface Model (DSM) is generated from the dense point cloud, representing the earth's surface and all objects on it.
9. Creating DTM: A Digital Terrain Model (DTM) is produced, which represents the bare earth surface without any objects like plants and buildings.
10. Creating Orthomosaic from RGB: An orthomosaic is created from the RGB images, offering a geometrically corrected, high-resolution image of the surveyed area.
11. Importing DEM: The Digital Elevation Model (DEM) is imported into the multispectral image project to ensure accurate elevation data is integrated.
12. Creating Orthomosaic for multispectral images: An orthomosaic is created for multispectral images, providing a detailed and accurate representation of the surveyed area in multiple spectral bands.
13. Calculating NDVI: The Normalized Difference Vegetation Index (NDVI) is calculated using the multispectral orthomosaic. This index is crucial for assessing vegetation health and density.

Results:

In terms of data processing, it should be considered that the height of the perspective center measurements is measured from ellipsoidal height which is geodetic height, and the height from RTK measurements are from geoid reference which is an orthometric height. What is more, the image coordinates of the perspective center are obtained without applying any corrections. As a result, the reliability of these measurements is reduced, and they are regarded as approximate values. Consequently, the emphasis is shifted towards the ground control points (GCPs), increasing their weight in the traditional bundle adjustment process.

In figure 2.18, it is shown that the RTK measurements for all eleven ground control points are not erroneous, and all of them can be considered as control points. In this figure, Z error is represented by ellipse color. X, Y errors are represented by ellipse shape.

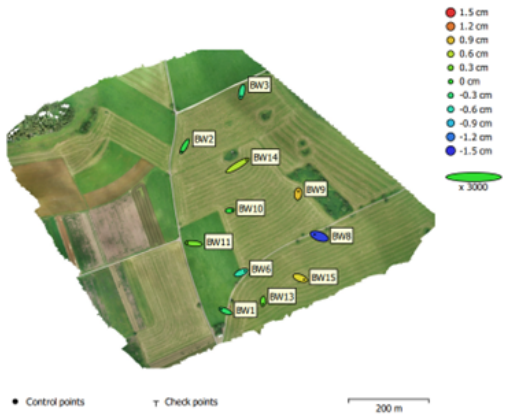

Figure 2.18: *Ground control points - error*

After processing images, the residuals on the GCPs are obtained as shown below in the table.

[H] Count	East (cm)	North (cm)	Height (cm)
11	0.697176	0.501225	0.63194

The accuracy of our RTK measurements for control points are around 2 cm, while the residuals are around 5 mm and 7 mm, which are consistent.
The project involved capturing a total of 923 images at a flying altitude of 76.1 meters, resulting in a ground resolution of 2.05 cm per pixel. The surveyed area coveres 0.522 square kilometers, with 923 camera stations utilized during the process. The data processing includes 423,936 tie points and 2,930,476 projections. The reprojection error is measured at 0.675 pixels. The camera calibration is depicted in figure 2.19.

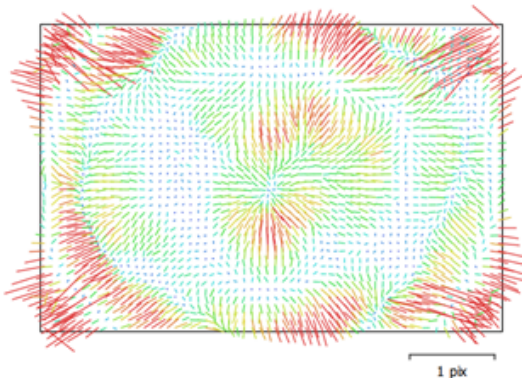

Figure 2.19: *Image residuals for FC6310R*

The Digital Terrain Model (DTM) and Digital Surface Model (DSM) are shown in figures 2.20 and 2.21, respectively. The Orthomosaic photo is also shown in figure 2.22. Creating the NDVI image involves a process that utilizes multispectral imagery to assess the presence and condition of vegetation in a given area. The NDVI image is shown in figure 2.23. For evaluation of the accuracy of DEM, two points are considered with known coordinates. With interpolation of the DEM, the height of the points are computed from DEM and it compared with the height of the RTK measurements.

[H] Points	Height differences (cm)
8	3.3
14	4.6

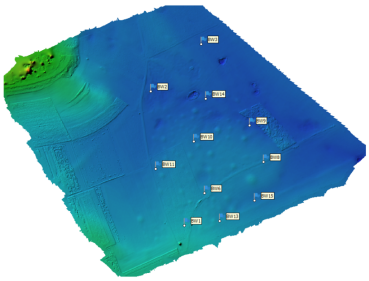

Figure 2.20: *Reconstructed DTM image*

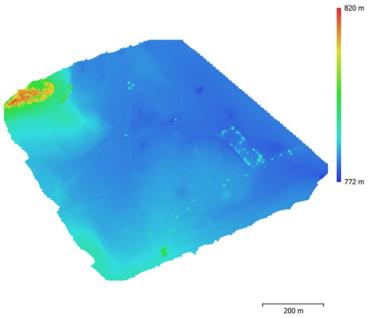

Figure 2.21: *Reconstructed DSM image*

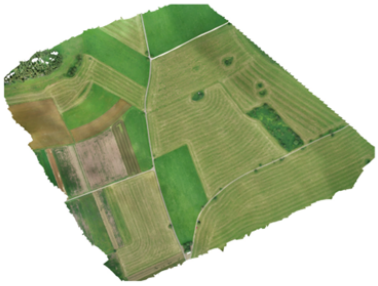

Figure 2.22: *Orthomosaic image*

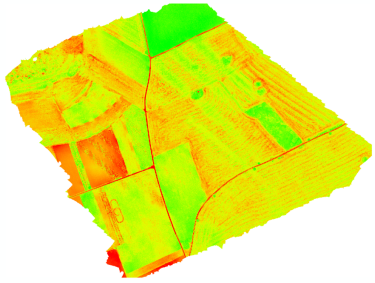

Figure 2.23: *NDVI image*

Height differences and magnetic fields: In the figures 2.24, 2.25 and 2.26 images illustrate the results of a geomagnetic survey and a digital surface model, a method used to detect and map subsurface features.

The first image is a color gradient map showing variations in height, with blue areas indicating low height and red areas indicating higher height. Red circles highlight specific anomalies, suggesting areas of interest due to buried features or geological structures.

The second image presents the same data in a grayscale magnetogram, where black areas represent positive magnetic changes and white areas represent negative changes. The contrast highlights magnetic anomalies more starkly, with red outlines indicating points of interest, possibly representing man-made structures or other subsurface features.

Together, these images provide a comprehensive view of the subsurface anomalies, aiding in identifying and interpreting magnetic changes due to height differences. Geomagnetic surveys are a non-invasive, effective method for archaeological and geological investigations, helping researchers plan fieldwork efficiently by focusing on areas with significant anomalies.

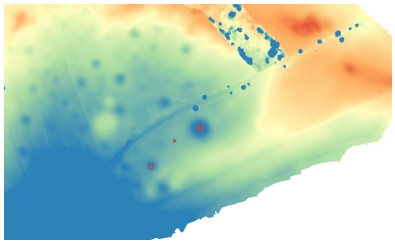

Figure 2.24: *Color gradient map showing variations in height*

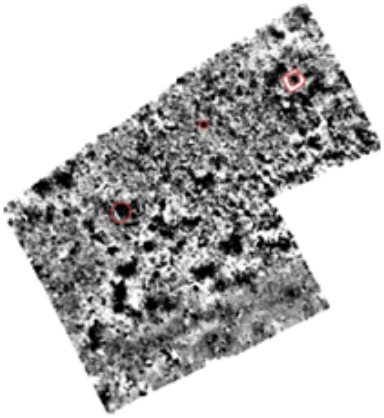

Figure 2.25: *Grayscale magnetogram*

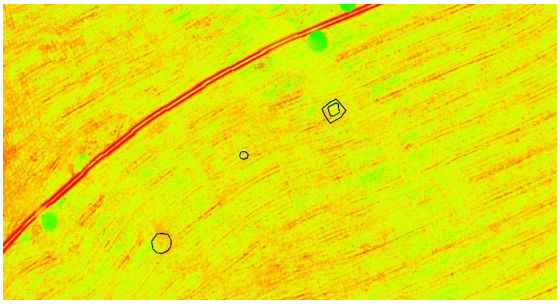

Figure 2.26: *Interest area of magnetic field on NDVI image*

2.5 Terrestrial laser scanning

Introduction

In addition to the drone images, a laser scanner measures the area of interest (burial mounds). With the point clouds received from laser scanning a surface model is created, which can be compared to the surface model of task 4. The reason for using laser scanner is a better measurement of height differences than with drone images.

Planning phase

The goal is to cover the whole area of Celtic burial mounds and then compare the calculated 3D surface model with the one of task 4.
For covering the entire area, six standing points for the laser scanner are needed resulting in six different point clouds. It is important to unify the different point clouds into one point cloud of the entire area. This can be achieved with black & white targets, which are positioned in three to four different directions of the scan area. In the software Leica Cyclone, which is used for post-processing, the black & white targets can be detected and compared.
To get a georeferencing the targets have to be measured as new points with total station. A free stationing between three to four reference points is needed. After free stationing the black & white targets can be changed to prisms and then measured as new points.

Figure 2.27: *Planned standing points of laser scanner*

Field Work

At first, the laser scanner Leica HDS7000 is built up on a tripod at the first planned standing point. The black & white targets are also built up with prism pole and mini tripod and well levelled on random points in the scan area. Then the instrument has

to be well levelled. After creating a new folder and scan, the desired accuracy and resolution is set to resolution as ”super high” and accuracy as ”high”. The scan takes 13 minutes and 28 seconds.
At the same time, the free stationing with total station is executed. First build up the instrument and level it on a different standing point than the laser scanner. Afterwards the prisms have to be built up and well levelled on four used reference points. As a next step, all settings like temperature, air pressure, number of rounds, name of standing point, name of aim point and prism heights in the controller of total station is entered and the prisms sighted out once. After that the automatically measurement starts. It is measuring two faces and three rounds.
When the laser scanner has finished its scan, the black& white targets have to be replaced by prisms. Then the total station measures all points as new points (again two faces and three rounds) and it calculates their coordinates. The same process is repeated on every of the six standing points.

Figure 2.28: *Laser scanner Leica HDS7000*

Evaluation and Results

Six different measurements are taken from the laser scanner to cover the focus area, highlighted in the red zone of the map (2.27). The next step is to import the data from the Laser Scanner to Leica Cyclone software to analyze and create a 3D model from the measurements. This step included registration via common black-and-white-targets (B&W targets) between each point cloud.

In the first part of analyzing the data using the aforementioned software by detecting the B&W targets either manually or automatically by algorithm, the automatic way does not work as expected. Then it is tried to manually detect the B&W targets but it faces challenges because the targets are not visible enough due to their distance of 110 meters from the laser scanner.
This problem leads to another issue with registering the point clouds. Normally, to combine two different point clouds from two different standing points, at least three common points or targets (B&W targets) are needed. In this case, only one common target is between each measurement which creates difficulties in merging the measurements.
Before moving to the next step, the coordinates of the B&W targets are taken from Leica Cyclone local coordinates of the Laser Scanner, aiming to be close to the middle of the target, with a worst-case offset of 4 cm. The purpose of taking the local coordinates is to transform them to global measurements using the total station, which would provide the transformation matrix. To georeference the point clouds, a transformation is needed to transform the local coordinates and apply the transformation matrix in the software to align the point clouds to global coordinates. However, this transformation plan does not work due to issues in JAG3D, which is the best plan in this case.
To proceed two options are possible. The first option is the Iterative Closest Point (ICP) algorithm, which estimates the rigid transformation between the moving and fixed-point clouds by minimizing the distance between the two-point clouds according to the specified metric. The data is shifted to Cloud Compare software and this method is aplied to two-point clouds. Despite multiple attempts, the results are not satisfactory due to insufficient overlapping between the point clouds (20%-30% overlap, whereas the ICP method requires 50%-60%).
The second option, though time-consuming, involves manually aligning the point clouds by choosing three common features and estimating the closest points. Aligning the Zainingen area as a point cloud is challenging due to the flat grass area lacking visible features. Additionally, each point cloud contains between 50 to 60 million points, which slows down the software significantly.

After aligning the six-point clouds together using Cloud Compare software, they are merged into one point cloud but the points are subsampled due to the software's slow performance. Subsampling is necessary, especially when dealing with almost 350 million points simultaneously. However, this process results in the loss of some features, as subsampling to 10 cm between each point, losing almost 70% of the points. Following this, a mesh is created using the Delauney 2D (XY plane) method on the merged point cloud, obtaining the initial surface model for Zainingen, as shown in the figures. To better visualize the Zainingen area and highlight the burial mounds, a scalar field to the merged mesh point cloud is applied, creating a Digital Elevation Model (DEM), as shown in the figures. To further understand the mounds, a filter is created to separate the ground points from non-ground points, making the mounds clearer. Then the ground

points are used and the scalar field is applied to see the elevations of the burial mounds more distinctly. By creating a Digital Terrain Model (DTM), the mounds are visualized in much greater detail compared to the DEM, as shown in the figures.

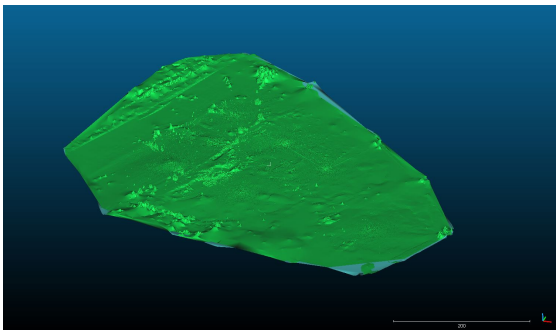

Figure 2.29: *Surface model*

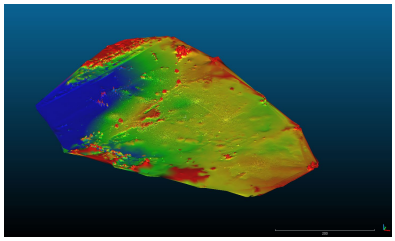

Figure 2.30: *DEM*

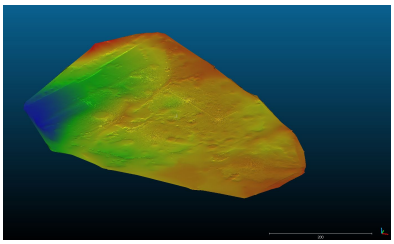

Figure 2.31: *DTM*

Conclusion: The evaluation highlights several challenges in data registration and alignment due to the distance and visibility of targets. Despite these obstacles, a detailed 3D model and visualizations of the Zainingen area are successfully created. Future work should focus on improving target visibility and overlapping during measurements to enhance the accuracy and efficiency of point cloud merging and analysis.

2.6 Kinematic GNSS data acquisition

Introduction

Global Navigation Satellite Systems (GNSS) are integral to numerous applications, from vehicle navigation to precise geodetic measurements. This task explores the use of GNSS for surveying with comparatively low-cost hardware, specifically focusing on a mobile multi-band Real-Time Kinematic (RTK) GNSS receiver mounted on a remote-controlled car, alongside a multi-band RTK reference station. The goal is to conduct height profiling of a designated area by utilizing this setup. The remote-controlled car, equipped with a Navio2 autopilot HAT running Manual, will provide real-time Single-Point-Position (SPP) data. Raw measurements collected will be stored for later processing converting into RTK data, enabling an assessment of the precision, accuracy, and practical advantages and limitations of using RTK GNSS technology in field surveys.

Planning phase

The Base station (Emlid Reach Rs2) is planned to be set up at a measured point, possible even a GNSS point, to compare the positioning with other measurements too. The Rover (Septentrio Mosaik X5 receiver + helix antenna) should start at the GNSS point Z2, following the road towards a levelling point 10004 and then perform a drive through a tree covered area to gather data within an obstructed area. Another, third static point should be T1, and after that a automatic drive should be performed in the area of interest (see fig. 2.32), using MissionPlanner.

Field Work

Within the field work, the Base station was positioned above point T5, free from surrounding trees. The measurements were otherwise performed as planned, with the different parts shown in the map: The remote-controlled car was driven manually along the planned route, starting from GNSS point Z2 and proceeding towards leveling point 10004.
The car navigated through the tree-covered area to gather data in regions with potential signal obstruction, ensuring comprehensive coverage.
The third point t1 was measured static when driving towards the field. All static points were measured 2min to easier find them in the dataset later.
The automatic drive was, because of a software sided problem, not possible. The Field (main area of interest) was therefore covered manually.

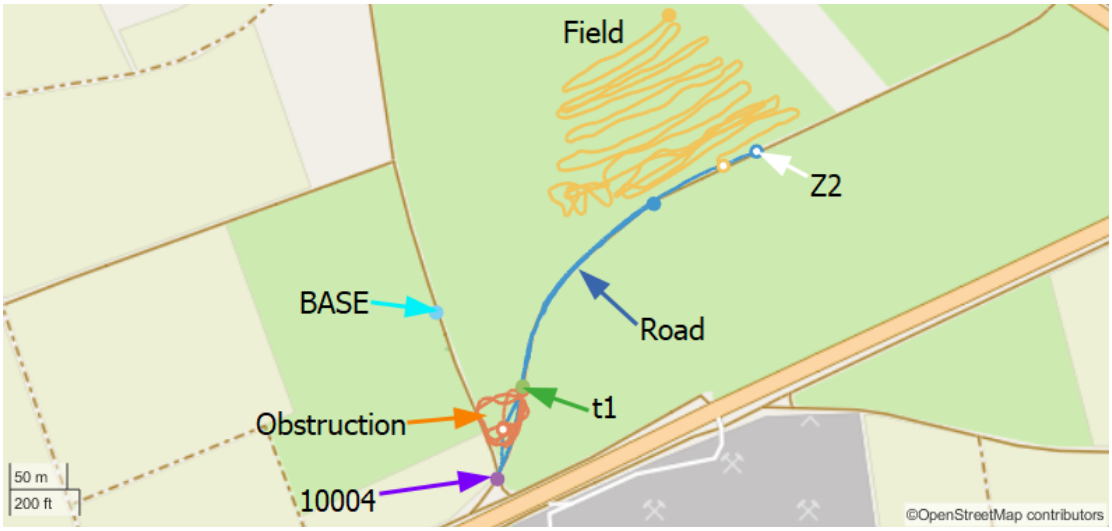

Figure 2.32: *Map (OpenStreetMap) of Task 6 measurements*

Evaluation and Results

The post-processing has been performed in RTKLIB [1] with the internal Geoid for the heights. For the transformation,[2] has been used with ETRS89 parameters [3]. All (Rover) heights have been corrected by the measured antenna height of 31.5 cm in the field.
In the first comparison, the Rover was single processed (SPP) for each static point and then with the base station (RTK).
Note: The processed Up values are listed under Height in the table and compared. Additional comments about that will be made in a later subsection.

SPP and RTK - static

Table 2.7: *Static measurement solutions*

Point		Mean East [m]	Mean North [m]	Mean h [m]	$\bar{\sigma}_E$ [m]	$\bar{\sigma}_N$ [m]	$\bar{\sigma}_U$ [m]
Z2	SPP	32541968.418	5370893.643	780.086	2.051	2.666	5.018
	RTK	32541967.203	5370892.032	778.681	0.003	0.003	0.006
t1	SPP	32541765.445	5370686.055	784.410	2.096	2.607	4.863
	RTK	32541764.087	5370684.917	782.243	0.003	0.003	0.006
10004	SPP	32541743.875	5370605.575	787.031	2.101	2.702	5.169
	RTK	32541742.439	5370604.061	785.137	0.003	0.004	0.006

As expected, SPP delivers measurements with accuracy in meters, the worst being the heights: Still the values for East and North are within 2 - 3 m and Height is at around 5 m. For SPP, values up to 10 m and more can be observed.
The RTK standard deviations are below centimeters and range from an average 3 mm for East and North to 6 mm for Height, which can be considered very accurate.
In a direct comparison, the actual SPP solution difference to RTK is below 2 m for

East/North at about 1.37 m and for Heights below 5 m with 1.82 m average.

SPP and RTK - kinematic
In case of the three kinematic measurements, the road and obstructed tree area

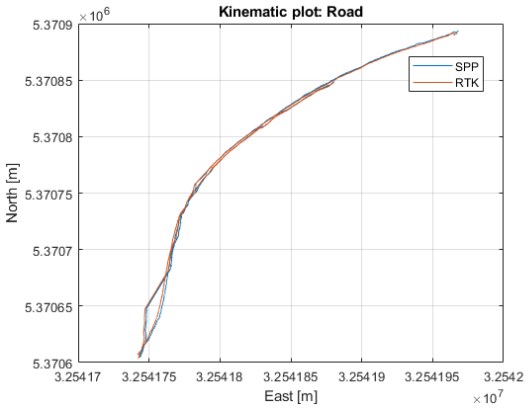

Figure 2.33: *SPP/RTK on Road*

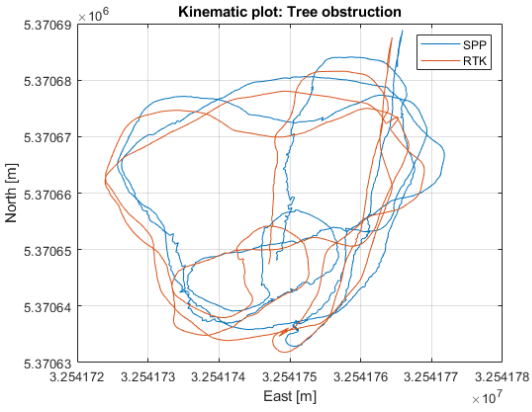

Figure 2.34: *SPP/RTK obstructed*

where compared giving the same results for the standard deviations as in the static SPP solution case, while only RTK got visibly worse when covered by trees by factor 3, now being within 1-2 cm for East/North and 2.3 cm for Height.

Table 2.8: *Kinematic measurement standard deviations*

Point		$\bar{\sigma}_E$ [m]	$\bar{\sigma}_N$ [m]	$\bar{\sigma}_U$ [m]
Road	SPP	2.093	2.670	5.032
	RTK	0.003	0.004	0.006
Trees	SPP	2.122	2.723	5.139
	RTK	0.012	0.016	0.023
Field	RTK	0.005	0.006	0.010

In the open kinematic scenario, RTK does not yield changes compared to the static scenarios too.
Both figures however show an offset between RTK and SPP. Comparing the 3D components separately in RTKLIB,

Figure 2.35: *Road: East, North and Height comparison RTKLIB SPP and RTK*

The road scenarios show a much smaller offset and smaller inaccuracies in the SPP solution (red, East first plot, North second plot), then when comparing it with the tree covered scenario.

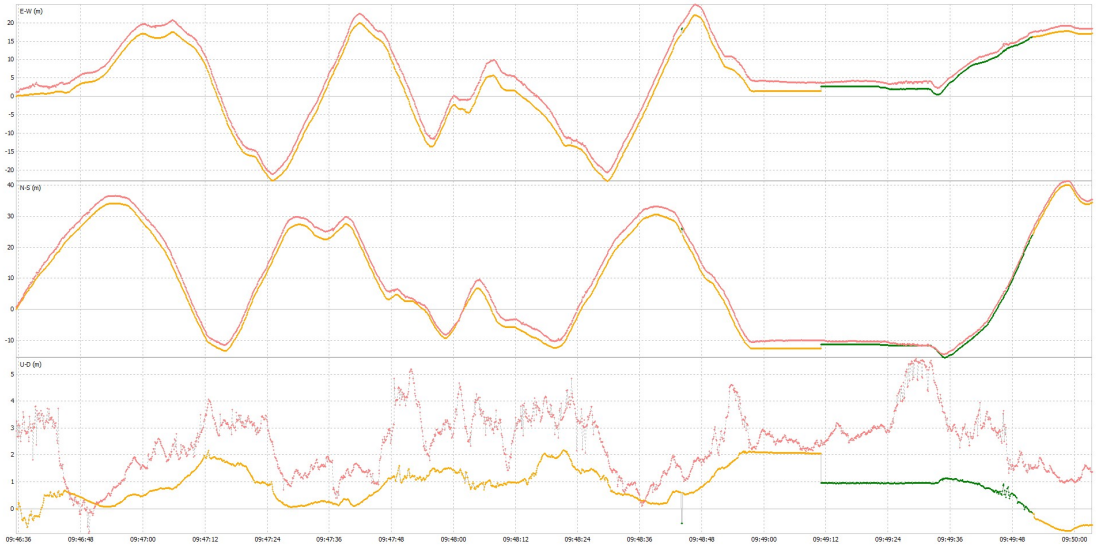

Figure 2.36: *Trees: East, North and Height comparison RTKLIB SPP and RTK*

Here, in case of the RTK plot (yellow and green), a loss of the fixed (green) solution can be observed for under the trees, only when circling out, a fixed solution was possible again. The last plot compares the Height solutions, where as to be expected RTK offers a much more stable solution.
Overall, the offset of SPP towards RTK can be observed in south and west direction.

RTK, Network and SAPOS

Comparing the RTK solution to the established network and SAPOS,

Table 2.9: *Static measurement comparison with network and SAPOS*

Point		Mean East [m]	Mean North [m]	Mean h [m]
t5	Base	34541687.843±1.0 cm	5370749.126±1.0 cm	-
	Network	32541687.8034	5370749.0787	781.0088
	SAPOS*	32541687.850	5370749.121	781.006
Point		**East [m]**	**North [m]**	**Height [m]**
Z2	Rover	32541967.203	5370892.032	778.681
	Network	32541967.2988	5370892.0373	779.5362
	SAPOS*	32541967.198	5370892.025	779.549
t1	Rover	32541764.087	5370684.917	782.243
	Network	32541764.0900	5370684.8341	783.1017
	SAPOS*	32541764.084	5370684.894	783.109
10004	Rover	32541742.439	5370604.061	785.137
	SAPOS*	32541742.391	5370604.022	786.046
** SAPOS threshold set to 2 cm*				

the Rover shows (abs.) differences in North/East up to almost 10 cm towards SAPOS only up to 5 cm in the last comparison (10004 was a levelling point and so not measured within the network), in any other case up to 2 cm. The Base station follows a similar pattern, being much closer to the SAPOS measurement (within about 1 cm). It is known that the network had difficulties and inaccuracies.
SAPOS was set to measure with a maximum of 2 cm precision, mostly measuring between 0.8-1.2 cm.

Heights

When it comes to heights, even after correcting the antenna height, an offset of around 85 cm (network) and 86-91 cm (SAPOS) can be observed towards the processed Up values: Note that in RTKLIB, the Geodetic height with internal Geoid was used (other models caused no output) and so an offset to the DHHN or any other local fitting Geoid and (orthometric) height system can be the reason for the offset towards a more general Geoid. Also, the antenna height was measured to the bottom of the helix antenna what could also lead to an offset to the actual center. Comparing the relative height differences between the levelling point 10004 and Z2

Table 2.10: *Height difference comparison*

Method	Δh [m]
levelling	-6.47844 m
Rover	-6.456 m
SAPOS	-6.497 m

the rover managed to measure with about 2.2 cm difference to the levelling (task 3) and 4.1 cm towards SAPOS. Especially the levelling comparison shows a accurate and to be expected difference in the height.

Automatic drive

Driving using MissionPlanner and a pre-defined route was not possible because of an unsolvable software error. The route above the area of interest, covering multiple of the Celtic graves, was then performed manually (see "Field" in fig. 2.32) and the processed data passed to task 4/5 for including them into their point clouds.

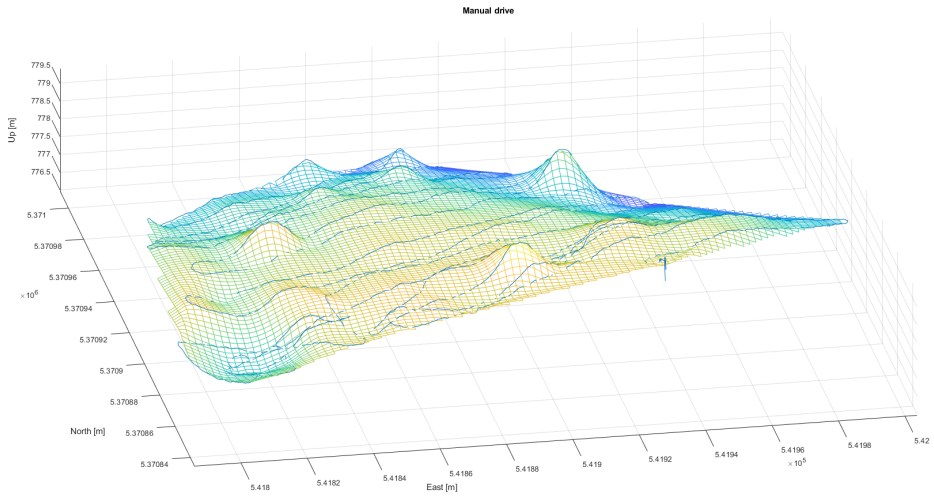

Figure 2.37: *3D plot of manual drive for point cloud comparison*

Conclusion

The RTK measurement delivered useful data especially in East/North even when obstructed by trees. The Height values need to be transformed additionally, or a functioning and suitable Geoid needs to be defined within RTKLIB. At least the relative height differences offer expected precision, yet are not comparable to a levelling measurement. However, for measurements as they are performed with SAPOS, e.g. measuring of properties outside of cities (fields, forest, construction planning) or for RTK based vehicle controlling (farming) the achieved previsions are suitable.

RESOURCES

1. RTKLIB demo5 b34j:
   https://github.com/rtklibexplorer/RTKLIB/releases
2. MATLAB function for transforming Lat/Lon to UTM:
   https://de.mathworks.com/matlabcentral/fileexchange/45699-ll2utm-and-utm2ll
3. ETRS89 parameters, last accessed 31/07/2024:
   https://en.wikipedia.org/wiki/European_Terrestrial_Reference_System_1989

3

Conclusion

In summary, this year's integrated internship was successful. All planned tasks were carried out under mostly good weather conditions and yielded satisfactory results, after sometimes lengthy troubleshooting. To verify the results, GNSS measurements were conducted using SAPOS, which confirmed the findings upon comparison.

In the first week, solutions for execution were found despite restrictions due to mowing activities. As in the first week, there were time constraints in the second week as well. On Wednesday of the second week, the State Office for Monument Preservation (LDA) came to conduct ground-penetrating radar measurements in the area.
The geophysicist from the LDA explained the method used, and we were able to take a look at the results, which showed a presumed structure beneath one of the burial mounds.

A control point network was successfully established in the measurement area. Based on this network, the area was subsequently surveyed geodetically.

UNIVERSIRY OF STUTTGART

REPORT FOR DONNSTETTEN

DONNSTETTEN, JULY 2024

0.1 List of students and supervisors

0.1.1 Students

- Brian Fleer
- Sourena Abdolzadeh
- Felix Bumiller
- MaedehSadat Jebelli
- Ali NouriEsfahani
- Liuqi Wang
- Huilin Wang

0.1.2 Supervisors

- James Foster
- Michael Cramer
- Ronja Miehling
- Gabriel Kerekes
- Ron Schlesinger
- David Collmar
- Lida Asgharian Pournodrati
- Vanessa Bär
- Clemens Sonnleitner

1

Introduction

1.0.1 Location

Donnstetten is a village located in the southern part of Germany, within the state of Baden-Württemberg. It is known for its historical significance, particularly due to the presence of an ancient Roman fort. This fort, situated at the southern border of Donnstetten, played a strategic role in the Roman Empire's defense system. The village and the fort are located at the geographical coordinates of approximately 48° 30′ 59.61" N latitude and 9° 33′ 45.81" E longitude.

1.0.2 History

Donnstetten, located in present-day Baden-Württemberg, Germany, is notable for its ancient Roman fort, which was discovered in 1975. This fort was part of the Roman Empire's defensive network, specifically protecting the Alb Limes—a boundary demarcating Roman territory. The site was identified through aerial surveys, which revealed distinct dark stripes in farmland, indicating the presence of fort ditches. The fort is strategically situated on a mountain plateau, naturally defended to the north by a 4-5 meter high rock chain. Although the site remains largely unexplored, it is significant for its historical importance as part of the Roman provincial system in Upper Germania and Raetia. The fort is set to be further investigated using ground-penetrating radar (GBR) as part of ongoing archaeological efforts.

1.0.3 Map

Roman Donnstetten The area around the Roman fort extends approximately 700 meters by 850 meters. However, the fort itself is much smaller, covering

only about 60 meters by 50 meters. This site is situated at the southern edge of the village of Donnstetten.

Figure 1.1: *Donnestetten*

1.0.4 Tasks

The IP 2024 project involved the comprehensive documentation and surveying of significant archaeological sites in Donnestetten. The primary objectives were to produce detailed 3D models of the sites, derive additional ortho photos and 2D maps, and prepare for the planning of visitor centers. We did this project in six separate tasks.

2

Tasks

In this chapter, we present a comprehensive overview of the six tasks completed in Donnstetten. Each task is described in detail, covering the planning phase, fieldwork, and evaluation of results. This structured approach ensures a clear understanding of our methodologies and findings.

2.1 Task 1

Introduction

This report presents the procedures and results of a GNSS survey conducted to determine precise coordinates for four unknown points (Z1,Z2,D1,D2). The survey utilized the static GNSS survey method, which involved multiple sessions of data collection using 8 GNSS receivers over a series of 1-hour sessions. The collected data was analyzed using Leica Infinity software to ensure high accuracy and reliability of the coordinates. Additionally, the height data was imported from a leveling task based on a known reference point to provide orthometric heights for the survey points .

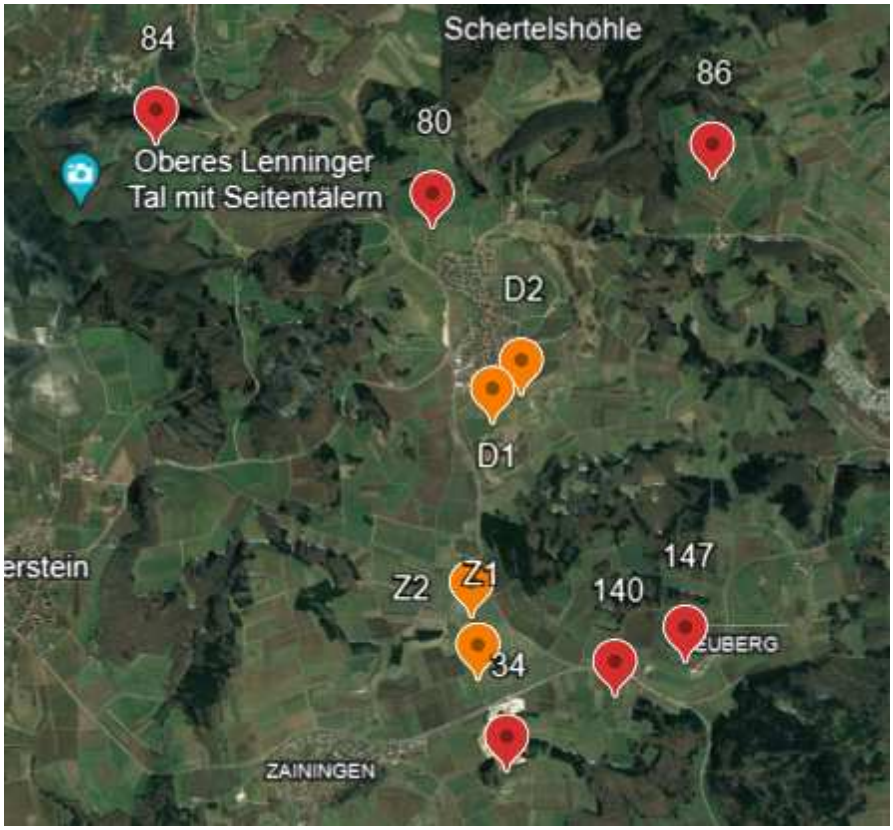

Figure 2.1: *Area Map*

Planning phase

Target: The primary goal of this survey was to obtain high-precision coordinates for a set of points using GNSS technology. This data is intended for determining coordinates for four unknown points which was needed for other tasks.

Equipment and Software: The following equipment and software were used during the survey:

- 8 Leica GNSS receivers
- Leica Infinity software
- Field controllers
- Tripods and tribrachs

Figure 2.2: *Leica AS10 GNSS Antenna*

Figure 2.3: *Leica GS15 GNSS Antenna*

Field Work

Survey Method:
The survey was conducted using the static GNSS survey method. The procedure involved the following steps:

1. Conducting 5 sessions of data collection, each lasting 1 hour.
2. Utilizing 8 GNSS receivers simultaneously to collect data.
3. Ensuring all receivers were properly calibrated and positioned at the survey points.

Evaluation and Results

Data Processing: The collected GNSS data was processed using the Leica Infinity software, following these steps:

1. Importing the raw GNSS data into the software.
2. Trimming the data to ensure a good overlap.
3. Processing the data to obtain preliminary coordinates.
4. Adjusting the network to refine the coordinates.
5. Analyzing the precision and accuracy of the results.

Results:
The final coordinates obtained from the survey are presented in the table below:

Table 2.1: *GNSS Survey Results – Coordinates and Measurement Precision*

Point ID	Easting (m)	Northing (m)	Height (m)	Std(E) (m)	Std(N) (m)	Std(H) (m)
Z2	32541967.188	5370892.006	779.403	0.003	0.004	0.008
Z1	32541626.540	5371041.210	777.596	0.005	0.007	0.014
D2	32542017.434	5373122.991	835.940	0.003	0.004	0.003
D1	32541820.510	5372891.011	813.110	0.003	0.004	0.003
147	32543318.150	5371121.740	832.478	0.000	0.000	0.010
141	32540628.712	5370357.031	814.671	0.005	0.007	0.014
86	32543849.530	5375185.330	839.873	0.000	0.000	0.010
84	32538941.821	5375099.300	781.666	0.002	0.003	0.006
80	32541212.180	5374571.600	819.568	0.000	0.000	0.029
34	32541902.260	5369974.390	862.523	0.000	0.000	0.005

Analysis of Results:
The analysis of the results indicates the following points regarding the accuracy and precision of the measurements:

- **Standard Deviations**: The small values of standard deviations (0.000 to 0.005 meters for Easting and Northing, and around 0.003 to 0.029 meters for height) indicate high precision in the measurements.
- **Consistency Across Measurements**: The consistency in standard deviation values across different points suggests reliable data collection and processing.

1. Observations:

- **No Significant Anomalies**: There are no significant anomalies in the data, as standard deviations are uniformly low.
- **Elevations**: The orthometric heights are consistent, with slight variations that are within the expected range of measurement error.

2. Data Interpretation:

- **Measurement Reliability**: The data indicates high reliability due to low standard deviations.
- **Application Suitability**: The precision of the measurements makes them suitable for high-accuracy applications such as geodetic control or detailed engineering surveys.

Future Improvements:

- Conduct more than five sessions to average out random errors and improve overall accuracy.
- Perform redundant measurements by placing additional GNSS receivers at the survey points. This can help in cross-verifying the data and identifying any discrepancies.

Potential Problems in the Field:

- Technical issues or human errors may cause some GNSS receivers to start recording data later than others, leading to inconsistencies in the dataset. Ensure all equipment is synchronized and functioning correctly before beginning the survey.
- Errors in measuring the height of the GNSS antenna above the survey point can lead to incorrect height calculations. Double-check the instrument height measurements to ensure accuracy.
- Signals reflecting off nearby structures or surfaces can cause multipath interference, affecting the accuracy of the measurements. Select survey sites with minimal potential for such reflections and use antennas with multipath mitigation technology.
- Poor satellite geometry (low PDOP values) can degrade the accuracy of the positioning. Schedule surveys when the satellite constellation is optimal, and monitor PDOP values during the survey.

Conclusion:
The GNSS survey successfully provided high-precision coordinates for the set of points under investigation. The analysis confirmed the reliability and precision of the measurements, with low standard deviations indicating minimal error. The results are suitable for applications requiring high accuracy, such as geodetic control and detailed engineering surveys. Future surveys may benefit from extended measurement durations and additional sessions to further enhance precision. Additionally, validating the GNSS-derived coordinates with known ground control points would strengthen the confidence in the survey results.

2.2 Task 2

Introduction

For the precise documentation of the archaeological site, it is necessary to establish a comprehensive three-dimensional (3D) network. A 3D network provides detailed and accurate information about the measurement area. Within the field, it should be possible to position ourselves with a Total Station to create and provide coordinates for future tasks, such as drone photogrammetry or terrestrial laser scanning. Total Stations are the preferred tool for such work because of their high precision and ability to measure both horizontal and vertical angles, as well as distances, with minimal error. The instrument we used in Task 2 was the Leica TS16

Planning phase

To establish a functional 3D network with Total Stations, careful planning is essential. Our network will consist of two datum points, which are precisely defined points on the Earth's surface used as references in geodetic systems. Additionally, fixed points are needed to densify the network. Together with the datum points, these fixed points allow for free stationing. For free stationing, at least three points are required, so it is important to ensure a clear line of sight to at least three points at all times. For higher accuracy, it is also crucial to position the fixed points as equidistantly and symmetrically as possible. A stable geometry in a 3D network ensures the highest level of accuracy.
First, it is important to consider where the datum points will be established. They should be well distributed across the field and not too close to each other, as this could significantly affect the accuracy of the fixed points.

In our case, these are points D1 and D2, which were also selected with a significant elevation difference to provide more stability in the Z-axis.
To position the fixed points (FP XX), a field inspection is necessary. This helps identify visual obstructions or other potential disturbances. The fixed points should facilitate free stationing within the area of interest and relate to the required points for other tasks. The locations of the fixed and datum points can be seen here:

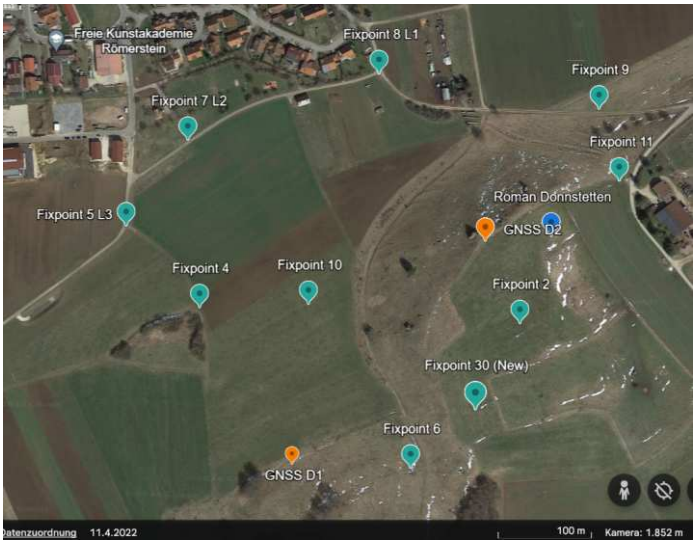

Figure 2.4: *Final Network Layout After Site Reconnaissance*

Table 2.2: *Overview of Points within our 3D-Network*

Typ	Name
Datum point	GNSS D1
Datum point	GNSS D2
Fixpoint	FP2
Fixpoint	FP30
Fixpoint	FP6
Fixpoint	FP10
Fixpoint	FP4
Fixpoint	FP5/L3
Fixpoint	FP7/L2
Fixpoint	FP8/L1
Fixpoint	FP9
Fixpoint	FP11

Field Work

For creating the network, some steps should be done:

1. **Marking the Points:**
   - Mark each survey point with wooden stakes.
   - Use ranging rods for additional visibility and marking precision.
2. **Setting Up the Total Station:**
   - Choose suitable locations for the total station to ensure clear visibility and coverage of all points.
   - Ensure the total station is leveled and securely positioned.
3. **Setting Up the Reflectors:**
   - Install reflectors at each of the fixed and datum points.
   - Confirm that each reflector is visible from the total station location and properly aligned.
4. **Performing Measurements:**
   - Conduct measurements using the total station, ensuring to perform five complete sets from each station point.
   - Verify the correctness of the station name before starting measurements to prevent data inconsistencies.
   - Record data systematically to ensure accuracy and repeatability.

A simple and initial network was defined before the fieldwork, which can be seen in Figure 2.5, and the final network can be seen in Figure 2.4. The network setup was revised with the following key differences:

- **Expansion of Network Points:** The number of points in the network increased from 8 to 12, enhancing coverage and measurement accuracy.
- **Relocation Towards Area of Interest:** Points were strategically shifted towards the area of interest to ensure more relevant and focused measurements.
- **Visibility Optimization:** The selection and positioning of points were optimized to minimize visibility obstructions to at least three points from any station, improving data reliability.
- **Inclusion of Height Reference Points:** Height fixed points on the road (L1, L2, L3) were incorporated into the network, aiding in precise elevation data collection.

Figure 2.5: *Initial Planned Network Layout Before Field Reconnaissance*

Evaluation and Results

The data analysis is performed using the tool Jag3D. This software allows for network adjustment, providing crucial information on accuracies, measurement errors, and the overall stability of the network.
At the beginning, the horizontal angles, vertical angles, and slant distances from all 9 stations are entered. Next, the datum points D1 and D2 are defined, the fixed points are designated as new spatial points, and the approximate coordinates are calculated. It's important to note that we are operating within our own local coordinate system. The uncertainties of the instrument should also be incorporated into the observations. You can download the datasheet for the Leica TS16 here. Once this is done, the first adjustment can be carried out.

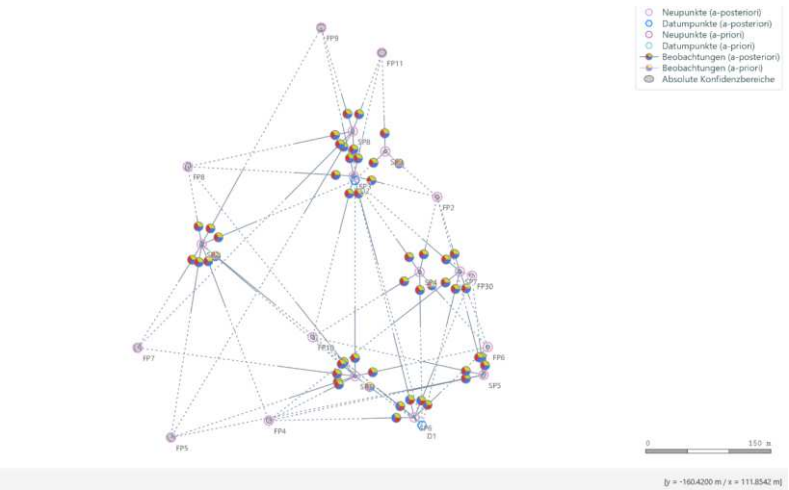

Figure 2.6: *Local Adjustment with all measurments*

Table 2.3: *Table of Components with all measurments*

Component	**n**	**r**	$1 \cdot \sigma^2$
Overall Adjustment	1614	1546.00	2126.78
Horizontal angle	538	507.25	160.48
Slope distance	538	520.81	271.02
Vertical angle	538	517.95	5918.47

Noticeable in this adjustment is the factor between the a-posteriori and a-priori variance in the zenith angles. Therefore, gross measurement errors must be present and need to be sorted out. In the next step, poor measurements are filtered out. This is possible due to our very good redundancy ratios.
To find the errors, the Baarda test (B-method) is applied. Subsequently, a filter is used to highlight all apriori data related to the test statistics in red, indicating those that did not pass the test.
If the factor between aposteriori and apriori for the individual components is below 1, the local adjustment can be considered complete. The global adjustment is performed by entering the real coordinates for D1 and D2, taking into account the accuracy of these coordinates. Subsequently, a new adjustment can be carried out, and we obtain coordinates for each fixed point in the UTM system.

Table 2.4: *Table of Global Adjustment*

Component	n	r	$1 \cdot \sigma^2$
Overall Adjustment	851	779.00	2.05
Horizontal Angle	291	263.80	0.99
Horizontal Angle σ_α	291	263.80	0.99
Slant Distance	385	364.18	0.56
Slant Distance σ_α	385	334.02	0.57
Slant Distance σ_c	385	30.16	0.50
Zenith Angle	169	149.03	0.94
Zenith Angle σ_α	169	149.03	0.94
Spatial Connection Point	6	1.99	495.91

First, the global coordinates of D1 and D2 with their accuracy after the adjustment:

Table 2.5: *The Coordinates of Datumpoints in Global System*

P.N	X (m)	Y (m)	Z (m)	σ_x (mm)	σ_y (mm)	σ_z (mm)
D1	32541820.4872	5372890.9220	813.2515	4.6	4.0	3.0
D2	32542017.4696	5373123.0460	836.0785	4.6	4.0	3.0

The global coordinates of fixed points with accuracies:

Table 2.6: *Coordinate and Accuracy Data of Fixed Points*

P.N	X (m)	Y (m)	Z (m)	σ_x (mm)	σ_y (mm)	σ_z (mm)
FP2	32542056.6510	5373030.4864	838.0715	5.1	3.1	3.0
FP4	32541721.5254	5373045.6402	796.0397	6.0	3.2	3.1
FP5	32541638.6083	5373130.9780	787.1513	7.4	4.1	3.1
FP6	32541942.3886	5372879.0257	825.5387	4.1	4.2	3.0
FP7	32541704.7769	5373224.6493	787.9106	6.2	4.7	3.1
FP8	32541918.0223	5373297.6601	792.8315	4.1	7.1	3.1
FP9	32542145.6929	5373259.7790	808.8061	6.5	6.4	3.1
FP10	32541833.6776	5373058.7499	801.1985	4.5	3.3	3.1
FP11	32542161.8942	5373182.7632	823.2967	6.7	4.9	3.0
FP30	32542002.0716	5372943.0017	831.3876	4.5	3.4	3.1

The final network in the global coordinate system can be seen in Figure 2.7.

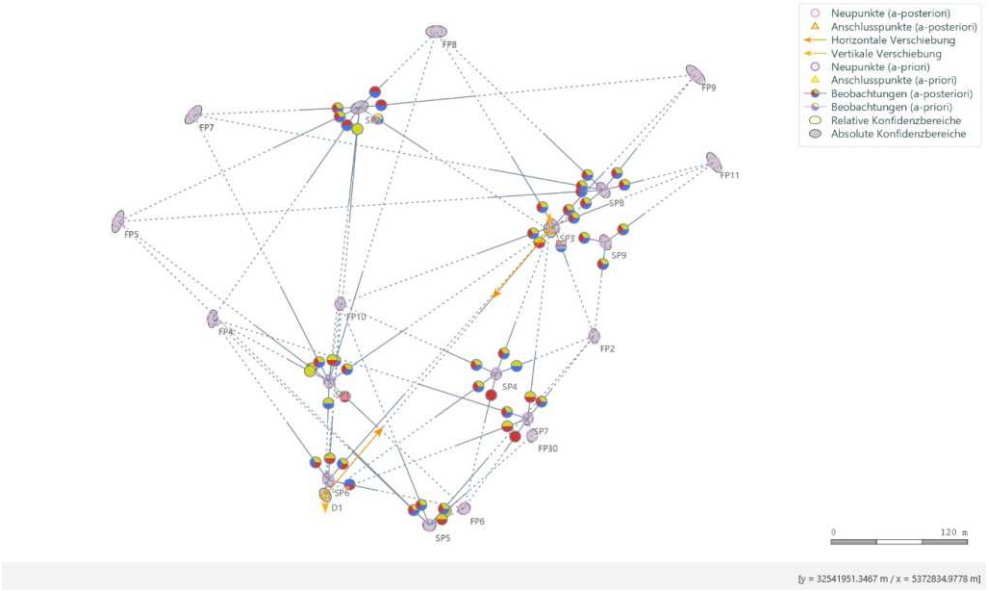

Figure 2.7: *Global Adjustment with all measurements*

We performed free stationing to evaluate the positional accuracy of three test standing points in the field. This approach allows us to precisely determine the positions and subsequently use these points for other tasks. The achieved accuracies for the test standing points are shown in Table 2.7. These accuracies are crucial for ensuring the reliability of subsequent measurements. The points determined through this method can then be used to acquire coordinates for additional points using polar measurements.

Table 2.7: *Field accuracies with test standing points*

Test Standing Point	Easting Quality (σ)	Northing Quality (σ)	Height Quality (σ)
TSP 1	5.5 mm	5.6 mm	1.4 mm
TSP 2	3.4 mm	3.5 mm	1.0 mm
TSP 3	10.2 mm	9.8 mm	0.0 mm

2.3 Task 3

2.3.1 Introduction

Geometric levelling determines height differences using horizontal sightlines between points close to each other. It involves a levelling instrument and two vertically positioned staffs. The height difference is calculated from the

readings taken at the back and foresights of the staffs. While geometric levelling is effective in many scenarios, it may not be practical for large height differences over short distances, such as steep hills or cliffs. In these cases, trigonometric levelling with Total Stations (TS) is used. This method involves measuring zenith angles between instruments to determine mounting heights. In creating networks with GNSS and TS observations, the Baden-Württemberg state network uses 2D coordinates for points. To accurately determine heights, geometric levelling or trigonometric levelling is employed based on the terrain. The instruments we used in Task 3 are: Trimble DiNi, Leica TS30 und Leica TS16.

(a) *Trimble DiNi*

(b) *Leica TS16*

Figure 2.8: *Comparison of Instruments*

2.3.2 Execution

The height difference between our target point and the known points is substantial, necessitating a two-step measurement approach to ensure precision and accuracy. Initially, we employ an electronic level to facilitate height transfer along the road. This method ensures the maintenance of accuracy over extended distances by minimizing potential cumulative errors associated with direct large height difference measurements.
In the second phase, we utilize a total station to determine the heights of points D1 and D2 through trigonometric levelling. Trigonometric levelling is particularly effective for accurately measuring significant height differences over shorter, more variable distances by using zenith angles and horizontal distances.
To enhance the precision of our measurements, we established three intermediate points along the road: L1, L2, and L3. These intermediate points serve to segment the overall height difference into smaller, more manageable increments, thereby reducing the likelihood of cumulative errors and improving

the accuracy of height transfer.
Following the establishment and measurement of intermediate points L1, L2, and L3 using the electronic level, we proceed with the second phase. Utilizing the total station, we conduct trigonometric levelling from these intermediate points (L1 and L2), as well as from the known points, to the target points D1 and D2. By accurately measuring the zenith angles and horizontal distances between these points, we can precisely calculate the relative height differences. Specifically, we form a height network by measuring from L1, L2, and the known points to the target points D1 and D2. This network helps in minimizing measurement errors by distributing them across multiple points, thus enhancing the overall accuracy of the height determination.
This two-step methodological approach, which integrates both electronic and trigonometric levelling techniques, ensures that our final height measurements are both precise and reliable. This is particularly crucial when dealing with challenging terrains characterized by significant elevation changes, where maintaining high measurement accuracy is imperative.

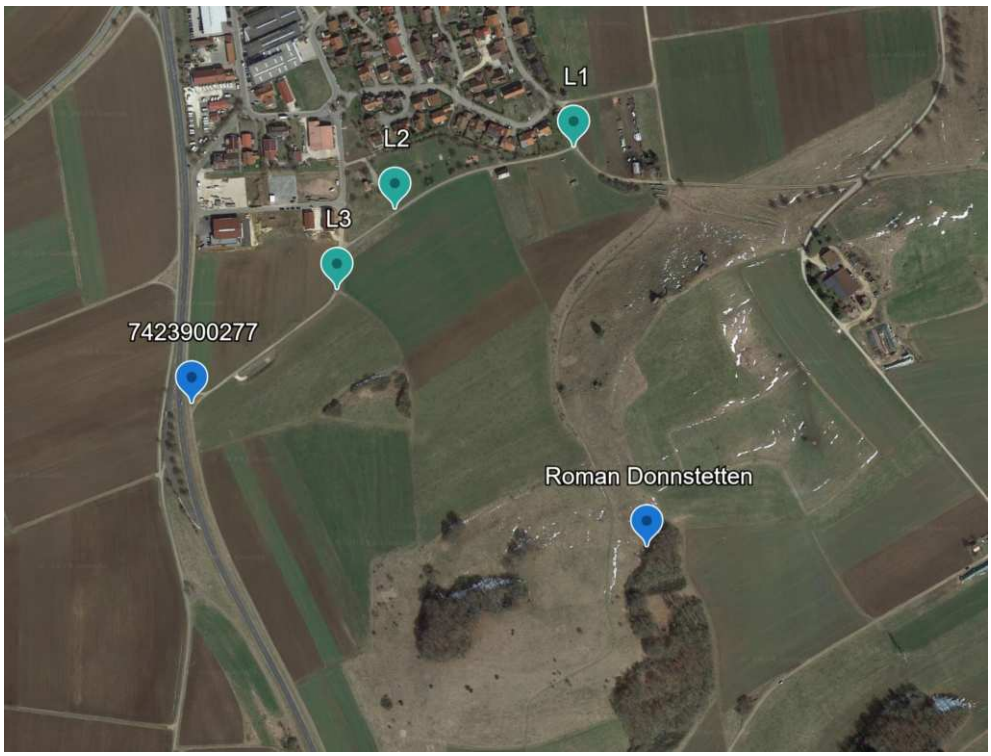

Figure 2.9: *build texture*

2.3.3 Part 1 - Levelling

We conducted leveling measurements in three segments between three intermediate points and known points. To ensure accuracy, we repeated the measurements. To meet accuracy requirements, the leveling closure error should be less than 1mm. The results are as follows.

Table 2.8: *Difference in altitude between 277 and L3*

Punktnr.	Blickrichtung	Höhendifferenz	Höhe
277			786.97600 m
277	Rb	1.54458 m	17.809 m
1	Rf	1.35170 m	17.600 m
1	Rf	1.35183 m	17.605 m
277	Rb	1.54466 m	17.807 m
1			787.17178 m
1	Rb	1.80444 m	29.828 m
2	Rf	1.55450 m	30.170 m
2	Rf	1.55447 m	30.156 m
1	Rb	1.80448 m	29.832 m
2			787.24625 m
2	Rb	1.50449 m	30.062 m
3	Rf	1.49183 m	29.921 m
3	Rf	1.49187 m	29.919 m
2	Rb	1.50434 m	30.060 m
3			787.44170 m
3	Rb	1.77064 m	30.154 m
L3	Rf	1.25381 m	29.803 m
L3	Rf	1.25389 m	29.802 m
3	Rb	1.77073 m	30.148 m
L3			787.26633 m
L3	Rb	1.25388 m	29.805 m
5	Rf	1.77072 m	30.149 m
5	Rf	1.77076 m	30.173 m
L3	Rb	1.25382 m	29.822 m
5			787.44186 m
5	Rb	1.52231 m	30.025 m
6	Rf	1.53452 m	29.965 m
6	Rf	1.53440 m	29.963 m
5	Rb	1.52222 m	30.017 m
6			787.24631 m
6	Rb	1.48913 m	30.020 m
7	Rf	1.73967 m	30.010 m
7	Rf	1.73966 m	30.012 m
6	Rb	1.48924 m	30.019 m
7			787.17179 m
7	Rb	1.34968 m	17.759 m
277	Rf	1.60895 m	17.613 m
277	Rf	1.60898 m	17.616 m
7	Rb	1.34973 m	17.755 m
277			786.97591 m

Table 2.9: *Difference in altitude between L3 and L2*

Punktnr.	Blickrichtung	Höhendifferenz	Höhe
L3			787.26633 m
L3	Rb	1.84555 m	30.087 m
1	Rf	1.21119 m	29.885 m
1	Rf	1.21066 m	29.897 m
L3	Rb	1.84530 m	30.085 m
1			787.90083 m
1	Rb	1.46264 m	17.069 m
2	Rf	1.41086 m	17.352 m
2	Rf	1.41083 m	17.352 m
1	Rb	1.46232 m	17.062 m
2			787.95247 m
2	Rb	1.62129 m	17.258 m
L2	Rf	1.53832 m	17.258 m
L2	Rf	1.53832 m	17.258 m
2	Rb	1.62115 m	17.256 m
L2			788.03537 m
L2	Rb	1.53879 m	17.245 m
5	Rf	1.62134 m	17.256 m
5	Rf	1.62140 m	17.258 m
L2	Rb	1.53840 m	17.253 m
5			787.95259 m
5	Rb	1.40829 m	17.159 m
6	Rf	1.45791 m	17.283 m
6	Rf	1.45806 m	17.279 m
5	Rb	1.40819 m	17.158 m
6			787.90285 m
6	Rb	1.19138 m	29.977 m
L3	Rf	1.82766 m	29.972 m
L3	Rf	1.82763 m	29.975 m
6	Rb	1.19122 m	29.972 m
L3			787.26650 m

Table 2.10: *Difference in altitude between L2 and L1*

Punktnr.	Blickrichtung	Höhendifferenz	Höhe
L2			788.03537 m
L2	Rb	1.97795 m	30.028 m
1	Rf	0.52120 m	30.020 m
1	Rf	0.52096 m	30.015 m
L2	Rb	1.97815 m	30.020 m
1			789.49234 m
1	Rb	2.33656 m	29.765 m
2	Rf	0.83387 m	30.124 m
2	Rf	0.83382 m	30.104 m
1	Rb	2.33658 m	29.798 m
2			790.99507 m
2	Rb	2.11182 m	29.889 m
3	Rf	1.05978 m	30.059 m
3	Rf	1.05979 m	30.056 m
2	Rb	2.11192 m	29.884 m
3			792.04715 m
3	Rb	1.89626 m	24.131 m
L1	Rf	0.99605 m	24.334 m
L1	Rf	0.99618 m	24.332 m
3	Rb	1.89630 m	24.131 m
L1			792.94732 m
L1	Rb	0.99600 m	24.334 m
5	Rf	1.89652 m	24.123 m
5	Rf	1.89633 m	24.136 m
L1	Rb	0.99609 m	24.334 m
5			792.04694 m
5	Rb	1.03749 m	29.852 m
6	Rf	2.08955 m	30.045 m
6	Rf	2.08958 m	30.036 m
5	Rb	1.03757 m	29.857 m
6			790.99490 m
6	Rb	0.84357 m	29.959 m
7	Rf	2.34520 m	29.949 m
7	Rf	2.34527 m	29.950 m
6	Rb	0.84366 m	29.963 m
7			789.49328 m
7	Rb	0.50211 m	29.959 m
L2	Rf	1.96028 m	29.966 m
L2	Rf	1.96020 m	29.968 m
7	Rb	0.50177 m	29.965 m
L2			788.03498 m

2.3.4 Part 2 - Trigonometric Levelling

Large height differences over short distances (e.g., steep hills or cliffs) cannot be determined by geometric levelling. In this case, trigonometric levelling with the total station (TS) will be performed. At our target points D1 and D2, and between the intermediate points L1, L2, and L3, due to large height differences over short distances, trigonometric levelling must be performed. To conduct trigonometric levelling, we will set up two total stations at the target points and intermediate points, respectively, and measure angles and distances between them simultaneously.

Figure 2.10: *build texture*

After measuring the horizontal distance and Zenith angles between two points simultaneously, use the following formula to calculate the height difference between the two points:

$$\Delta h = \frac{1}{2} S_H \cdot (\cot Z_1 - \cot Z_2) + (i_1 - i_2) + (t_1 - t_2)$$

where:

- Δh is the height difference between the two points.

- S_H is the horizontal distance between the two points.
- Z_1 is the Zenith angle at the first point.
- Z_2 is the Zenith angle at the second point.
- i_1, i_2 are the instrument heights at each station point.
- t_1, t_2 are the target heights in each case.

Offsets between the instrument center and reflector (verify if needed):

- Leica TS30: 0.286 m
- Leica TS16: 0.275 m

Table 2.11: *calculated height difference results*

	GNSS	Levelling	Δ
D1-L2	25.07463 m	25.05074 m	0.02389 m
D1-L4	26.13400 m	26.07223 m	0.06177 m
D2-L1	42.99268 m	42.84802 m	0.14466 m

2.3.5 Evaluation Result

Levelling

We used Jag3d to adjust the results of leveling measurements. JAG3D performs leveling data adjustment based on the principle of least squares, minimizing the total error to obtain the best estimates. This process provides not only the adjusted elevations but also error estimates and residual analysis, used to evaluate the quality and reliability of the observation data.

The results of the adjustment between Station 277 and L3:

Table 2.12: *Adjustment Results between Station 277 and L3*

Station-Id	Target-Id	δh in m	σh in mm	r in %	ϵ in mm	V in mm	V(1) in mm	V(λ) in mm
277	1	0.1958	0.0	8.89	0.0	-0.1	-0.7	-3.0
1	2	0.0745	0.0	13.71	0.0	-0.1	-0.7	-3.0
2	3	0.1955	0.0	13.70	0.0	-0.1	-0.7	-3.0
3	L3	-0.1754	0.0	13.70	0.0	-0.1	-0.7	-3.0
L3	5	0.1755	0.0	13.70	0.0	-0.1	-0.7	-3.0
5	6	-0.1955	0.0	13.70	0.0	-0.1	-0.7	-3.0
6	7	-0.0745	0.0	13.71	0.0	-0.1	-0.7	-3.0
7	277	-0.1959	0.0	8.88	0.0	-0.1	-0.7	-3.0

Table 2.13: *Error Propagation and Statistical Parameters between Station 277 and L3*

EP in mm	EF·SPmax in mm	Ω	log(Pprio)	log(Ppost)	Tprio	Tpost
-0.1	0.0	0.0	-0.11	0.00	0.02	0.00
-0.1	0.0	0.0	-0.11	0.00	0.02	0.00
-0.1	0.0	0.0	-0.11	0.00	0.02	0.00
-0.1	0.0	0.0	-0.11	0.00	0.02	0.00
-0.1	0.0	0.0	-0.11	0.00	0.02	0.00
-0.1	0.0	0.0	-0.11	0.00	0.02	0.00
-0.1	0.0	0.0	-0.11	0.00	0.02	0.00
-0.1	0.0	0.0	-0.11	0.00	0.02	0.00

The results of the adjustment between L3 and L2:

Table 2.14: *Adjustment Results between L3 and L2*

Station-Id	Target-Id	δh in m	σh in mm	r in %	ϵ in mm	V in mm	V(1) in mm	V(λ) in mm
L3	1	0.6345	0.1	22.02	-0.0	0.2	0.6	2.3
1	2	0.0516	0.1	13.98	-0.0	0.2	0.6	2.3
2	L2	0.0829	0.1	14.01	-0.0	0.2	0.6	2.3
L2	5	-0.0828	0.1	14.00	-0.0	0.2	0.6	2.3
5	6	-0.0498	0.1	13.98	-0.0	0.2	0.6	2.3
6	L3	-0.6364	0.1	22.01	-0.0	0.2	0.6	2.3

Table 2.15: *Error Propagation and Statistical Parameters between L3 and L2*

EP in mm	EF·SPmax in mm	Ω	log(Pprio)	log(Ppost)	Tprio	Tpost
0.1	0.0	0.02	-0.27	0.00	0.09	0.00
0.1	0.0	0.01	-0.27	0.00	0.09	0.00
0.1	0.0	0.01	-0.27	0.00	0.09	0.00
0.1	0.0	0.01	-0.27	0.00	0.09	0.00
0.1	0.0	0.01	-0.27	0.00	0.09	0.00
0.1	0.0	0.02	-0.27	0.00	0.09	0.00

The results of the adjustment between L2 and L1:

Table 2.16: *Adjustment Results between L2 and L1*

Station-Id	Target-Id	δh in m	σh in mm	r in %	ϵ in mm	V in mm	V(1) in mm	V(λ) in mm
L2	1	1.4570	0.1	13.05	0.1	-0.4	-0.7	-3.0
1	2	1.5028	0.1	13.05	0.1	-0.4	-0.7	-3.0
2	3	1.0521	0.1	13.04	0.1	-0.4	-0.7	-3.0
3	L1	0.9002	0.1	10.90	0.0	-0.4	-0.7	-3.0
L1	5	-0.9003	0.1	10.90	0.0	-0.4	-0.7	-3.0
5	6	-1.0520	0.1	13.03	0.1	-0.4	-0.7	-3.0
6	7	-1.5016	0.1	13.03	0.1	-0.4	-0.7	-3.0
7	L2	-1.4582	0.1	13.03	0.1	-0.4	-0.7	-3.0

Table 2.17: *Error Propagation and Statistical Parameters between L2 and L1*

EP in mm	EF·SPmax in mm	Ω	log(Pprio)	log(Ppost)	Tprio	Tpost
-0.3	0.2	0.04	-0.52	0.00	0.28	0.00
-0.3	0.2	0.04	-0.52	0.00	0.28	0.00
-0.3	0.2	0.04	-0.52	0.00	0.28	0.00
-0.3	0.2	0.03	-0.52	0.00	0.28	0.00
-0.3	0.2	0.03	-0.52	0.00	0.28	0.00
-0.3	0.2	0.04	-0.52	0.00	0.28	0.00
-0.3	0.2	0.04	-0.52	0.00	0.28	0.00
-0.3	0.2	0.04	-0.52	0.00	0.28	0.00

Trigonometric Levelling

To evaluate the results of Trigonometric levelling, it is necessary to use the covariance matrix because it measures the uncertainty and reliability of the estimated parameters. The covariance matrix quantifies variances and covariances between measurements, allowing for accurate error analysis and quality assessment of the data. This ensures reliable and accurate results in the surveying process.

Covariance matrix formula:

$$\Sigma_H = F \cdot \Sigma_{ZS} \cdot F' \tag{2.1}$$

F Error propagation matrix:

$$F = \begin{bmatrix} \frac{\partial H_1}{\partial s^R_{1\,1}} & \frac{\partial H_1}{\partial z_{11}} & \frac{\partial H_1}{\partial s^R_{2\,1}} & \frac{\partial H_1}{\partial z_{21}} & 0 & 0 & 0 & 0 & 0 & \cdots \\ 0 & 0 & 0 & 0 & \frac{\partial H_2}{\partial s^R_{1\,2}} & \frac{\partial H_2}{\partial z_{12}} & \frac{\partial H_2}{\partial s^R_{2\,2}} & \frac{\partial H_2}{\partial z_{22}} & 0 & \cdots \\ \vdots & \vdots & \vdots & \vdots & \vdots & \vdots & \vdots & \vdots & \vdots & \vdots \\ 0 & 0 & 0 & 0 & 0 & 0 & \frac{\partial H_{10}}{\partial s^R_{1\,10}} & \frac{\partial H_{10}}{\partial z_{1\,10}} & \frac{\partial H_{10}}{\partial s^R_{2\,10}} & \frac{\partial H_{10}}{\partial z_{2\,10}} \end{bmatrix}$$

$$\sigma_H = \sqrt{diag(\Sigma_H)}$$

Standard deviation of Trigonometric levelling D2 and L1:

$$\sigma_H = 0.5498mm$$

Standard deviation of Trigonometric levelling D1 and L2:

$$\sigma_H = 0.8680mm$$

Standard deviation of Trigonometric levelling D1 and 277:

$$\sigma_H = 0.8994mm$$

These standard deviations reflect the precision of the levelling measurements between the respective points, with smaller values indicating higher precision. This indicates that the measurement accuracy is high and meets the required standards.

2.4 Task 4

Introduction

Drone photogrammetry represents a significant advantage in the field of spatial data collection and analysis. The significance of drone photogrammetry lies in its ability to provide rapid and accurate data acquisition over large areas with minimal human intervention. Traditional photogrammetry methods often require extensive ground control and manual measurements, whereas drones can cover difficult-to-access areas safely and efficiently. These advantages provide an opportunity to use it in different areas such as:

- Construction: Monitoring construction progress, site planning, and volume calculations.
- Environmental Monitoring: Tracking changes in landscapes, deforestation, and coastal erosion.
- Surveying and Mapping: Creating topographic maps, land surveys, and infrastructure assessments.
- Heritage Documentation: Generating detailed 3D models for heritage sites.

As it was mentioned, one of the applications of photogrammetry is heritage documentation, which is the main focus of this project which will be explained in detail later. Moreover, running a photogrammetry project needs different steps which are done before, meanwhile, and after the project. The mythology of drone photogrammetry can be divided into five steps:

1. Flight Planning: The first step involves designing a flight plan to ensure optimal coverage and overlap of the area to be surveyed. This includes determining flight altitude, speed, flight lines, number of images, GSD etc.
2. Image Acquisition: During the flight, the drone captures a series of overlapping images. The camera, quality of images,
3. Georeferencing: Each image is tagged with GPS coordinates, allowing for accurate spatial positioning. Ground control points (GCPs) may be used to enhance accuracy.
4. Image Processing: Specialized photogrammetry software (Agisoft Metashape) processes the images to create a 3D point cloud, from which digital elevation models (DEMs), orthomosaics, and other spatial data products are derived.

5. Data Analysis and Interpretation: The final step involves analyzing the processed data to extract meaningful information relevant to the specific application. This can include measurements, volume calculations, change detection, and more. For this project, the DEM, NDVI map and orthomosaics are desired outcomes.

In the next part, an overview of the project is provided.

Planning phase

For implementing task 4 of the photogrammetry project, a planning phase is necessary to check the required instruments and their specifications. The most important instrument is the DJI Phantom 4 RTK, which is equipped with the standard DJI Zenmuse FC6310R (Figure 2.5). The image size is 5472 x 3648 pixels, the pixel size on the sensor is 2.4 mm, and the focal length is 8.8 mm. The coordinate of each perspective center is measured with a GNSS antenna.

Figure 2.11: ***The DJI Phantom 4 with DJI Zenmuse camera (Souta Outdoor. 2024).***

Another camera is the Parrot Sequoia multi-spectral camera (Figure 2.6) has five channels for producing NDVI or false color maps. The image size is 1280 x 920 pixels, the pixel size on the sensor is 4.9 mm, and the focal length is 3.98 mm. Finally, for control points 15 checkered plates are used (Figure 2.7).

Figure 2.12: *The Parrot Sequoia Mutli-Spectral Camera (Souta Outdoor. 2024).*

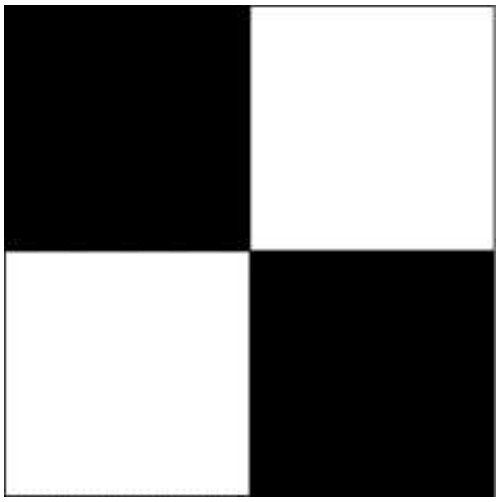

Figure 2.13: ***The Checkered Control Point.***

Flight Planning Considerations

Effective drone photogrammetry requires careful flight planning. The following considerations were taken into account:

- **Area of Interest:** Define the boundaries and extent of the area to be surveyed.
- **GSD Size:** Set the desired Ground Sampling Distance, with 2 cm for the RGB camera and 5 cm for the multispectral camera.
- **Flight Height:** Maintain a consistent flight altitude, not exceeding 120 meters, to ensure data quality and safety. The flight altitude of 75m was realized.

- **Overlap:** Ensure sufficient image overlap for accurate stitching and processing. Use 80% front overlap and 60% side overlap for the RGB camera, and 80% front overlap with 30% side overlap for the multispectral camera.
- **Safety Precautions:** Avoid flying over populated roads, and inform any affected locals in advance.
- **Control Points:** Use 15 ground control points, with adjustments made as necessary to account for large height differences or other issues.
- **Sensor Size:** Consider the sensor sizes, with 2.4 µm for the RGB camera and 4.9 µm for the multispectral camera.
- **Flight Speed:** Prefer lower flight speeds to minimize motion blur.

With this information, the performed flight planning should be done which can be seen in Figure 2.14.

Figure 2.14: *The Performed Flight Performed (perspective center coordinates shown)*

Field Work

After preparing the flight planning with considerations, the drone flight should be done. Before drone flight, the position of ground control points should be distributed in the area of interest. 15 control points are used for forming the network and georeferencing and evaluating the accuracy over the checkpoints. The distribution of control points can be seen in Figure 2.15. It should be mentioned that the ground control points are measured with RTK. After fixing and measuring the control points, the drone flight was done.

Figure 2.15: *The Distribution of Ground Control Points.*

Evaluation and Results

After the drone flight, the collected data was evaluated and processed. Before presenting the results, several important points regarding the processing steps and input data need to be addressed:

1. The perspective centre image coordinates did not undergo corrections during measurement. Therefore, the weight assigned to these measurements was decreased, treating them as approximate values. Conversely, the weight of the ground control points was increased to rely more heavily on the traditional bundle adjustment. It was a single point positioning solution for the drone trajectory, which always refers to ellipsoidal heights with accuracy in the range of a meter.
2. The height of the perspective center measurements was recorded as ellipsoidal height (geodetic height), whereas the RTK measurements provided heights based on the geoid (orthometric height). To convert these heights into a single reference system, a geoid model is required, which was not accessible via Agisoft Metashape and was only available on a specific computer in the field.
3. A comparison of the control points from the 3D network and RTK measurements revealed significant differences. The coordinates of these points are presented in Table 2.18.
4. Some RTK measurements for control points are erroneous. This was concluded from their reprojection of the images and the software's survey statistics. The reprojection error of one of the points is illustrated in Figure 2.16. The bundle adjustment provides an opportunity to examine the quality and accuracy of GCP.

Table 2.18: *The RTK Measurements and 3D Terrestrial Network*

Point Number	Easting (m)	Northing (m)	Height (m)
3	0.0860	0.1140	0.2030
7	0.0970	0.1010	0.1950
12	0.0290	0.0530	0.1810

Figure 2.16: *The Erroneous Point (Number 5)*

The error ellipsoid of the erroneous points can be seen in Figure 2.17.

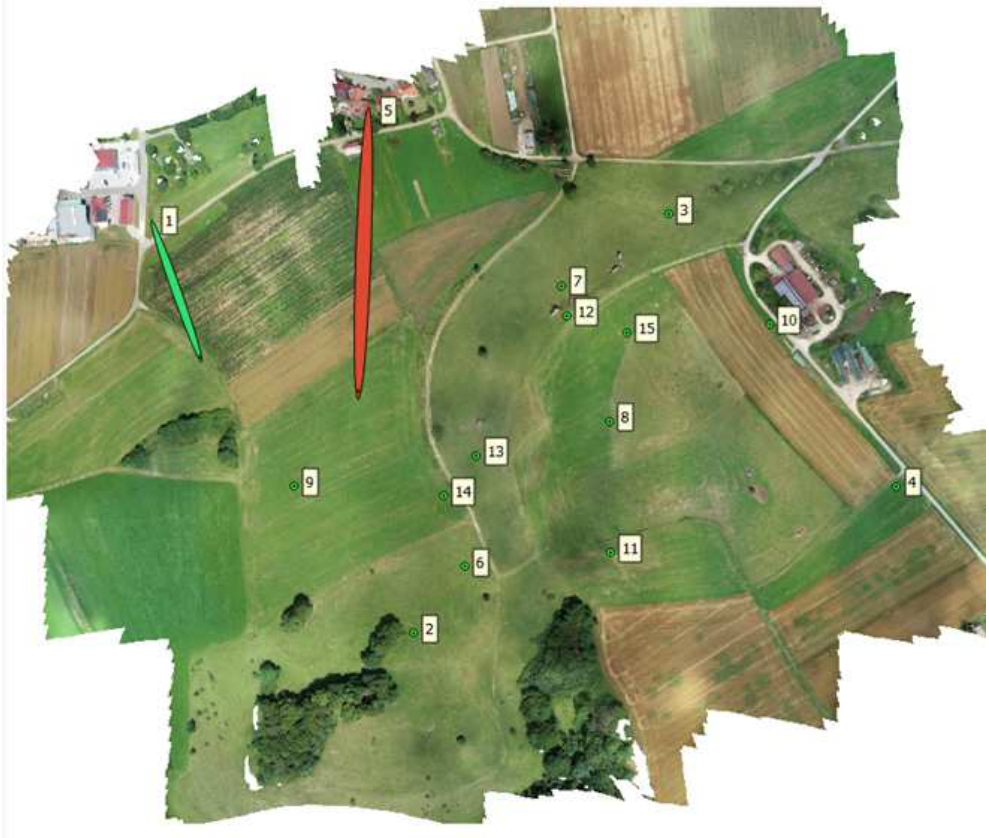

Figure 2.17: *The Error Ellipsoids of the Erroneous Points*

With consideration of the mentioned problems and tackling them with different approaches, the results are processed. To be consistent in producing the results, the residuals on the control points (11 points) and checkpoints are evaluated, which can be seen in Table 2.19. Two points which are not erroneous are considered checkpoints (points number 12 and 14). Some of the details for the processing can be seen in Figure 2.18. The camera residuals can be seen in Figure 2.19.

Table 2.19: *The Accuracy of the Checkpoints and Residuals on the Control Points*

Points	Easting (m)	Northing (m)	Height (m)
Checkpoints	0.0112	0.0142	0.0017
Control Points	0.0004	0.0003	0.0006

The GSD for the project is 2cm. With a comparison between GSD and the accuracy and residuals, the desired accuracy is achieved.

Number of images:	792	Camera stations:	792
Flying altitude:	124 m	Tie points:	349,529
Ground resolution:	2.87 cm/pix	Projections:	2,616,436
Coverage area:	0.484 km²	Reprojection error:	0.722 pix

Figure 2.18: *Details of Processing*

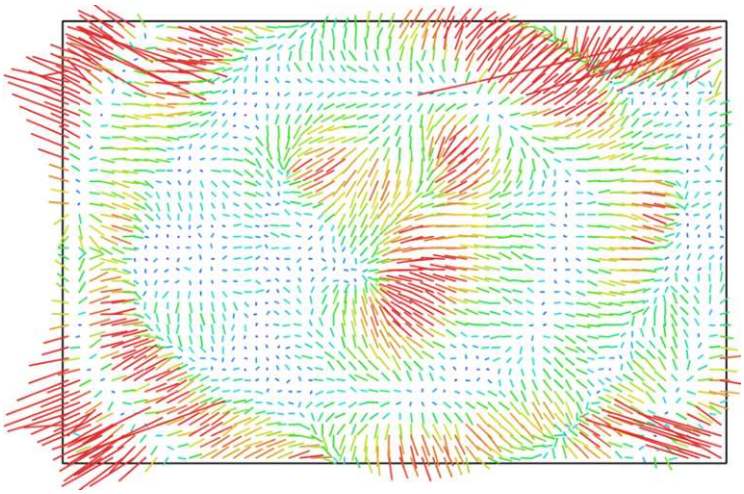

Figure 2.19: *The Camera Residuals*

The project's desired results were DEM, DSM, point cloud, NDVI map, and orthomosaic. For processing, the bundle adjustment should first be done with ground control points and perspective centre approximation coordinates.

Then, the dense image machining should be done, and the point cloud, the mesh, DEM, DSM and orthomosaic should be created. The point cloud can be seen in Figures 2.20 and 2.21. And also the DEM can be seen in Figure 2.22.

Figure 2.20: *The Point Cloud from first View*

Figure 2.21: *The Point Cloud from the second View*

For evaluating the accuracy of DTM, two points D1 and D2 with known height

from the levelling part were used to determine the height differences between them and DTM. The differences can be seen in Table 2.20.

Table 2.20: *Evaluation of DSM Accuracy*

Point Number	Differences (cm)
D1	0.04
D2	0.03

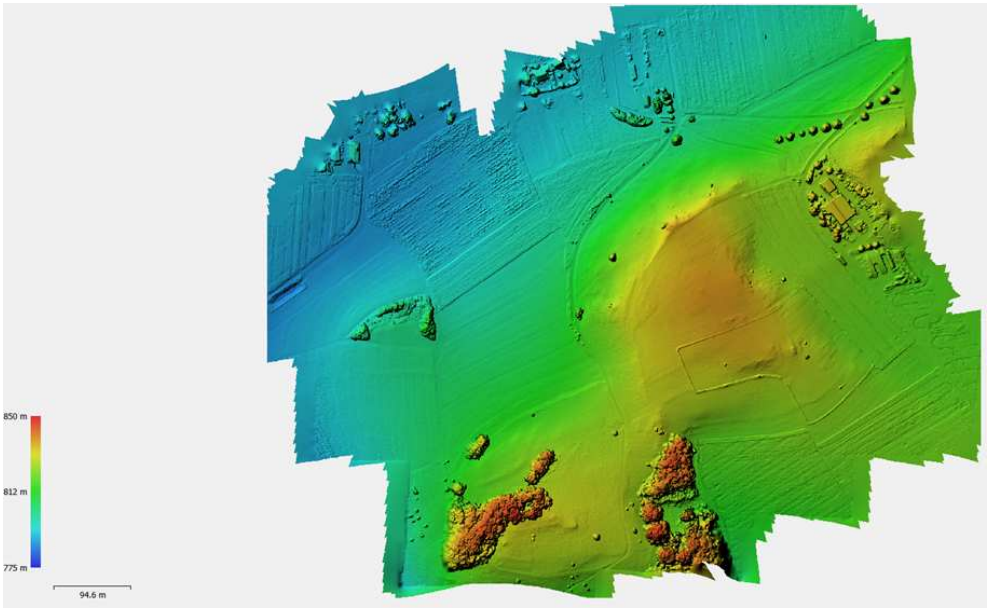

Figure 2.22: *The Digital Elevation Model*

With classification of points in DEM, the DSM is provided in Figure 2.23.

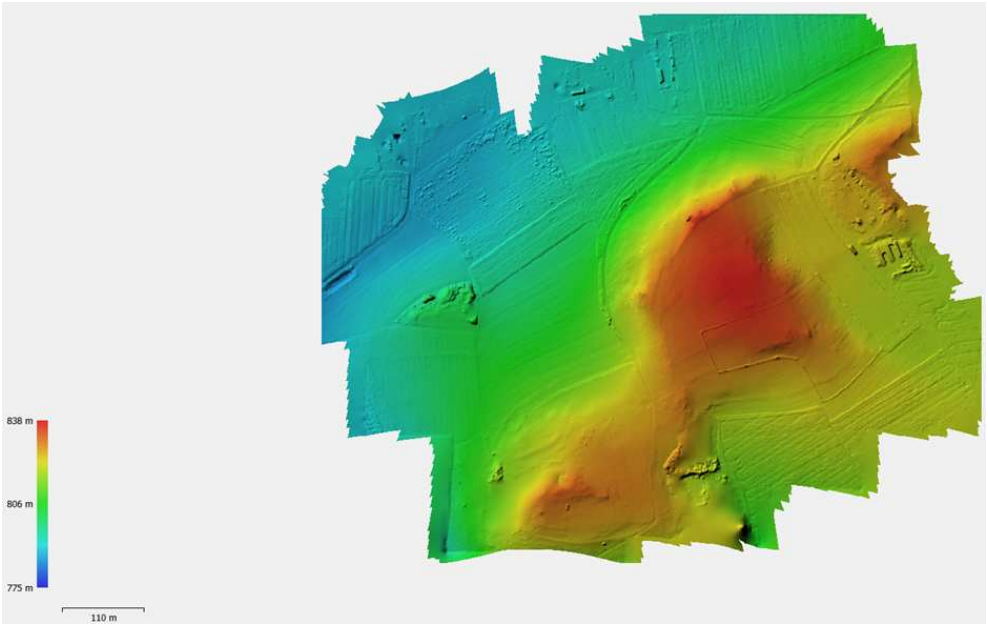

Figure 2.23: *The Digital Surface Model*

The orthomosaic photo can be seen in Figure 2.24.

Figure 2.24: *The Orthomosaic of the Area from RGB imagery*

For the final part, the NDVI map should be provided, which is created with a combination of Red and Near Infrared bands. The orthomosaic for each channel is created and georeferenced with ground control points. The result of the NDVI map can be seen in Figure 2.25. The NDVI map is calculated

with the subtraction of NIR and Red in the numerator and divided by their summation. In the laser scanner data, more gaps can be seen in the flat area, whereas in the rock images, the gaps between the rocks are more. It should be considered that the drone images are captured from a nadir view. Thus, their accuracy would be better for the flat area which are detected better.

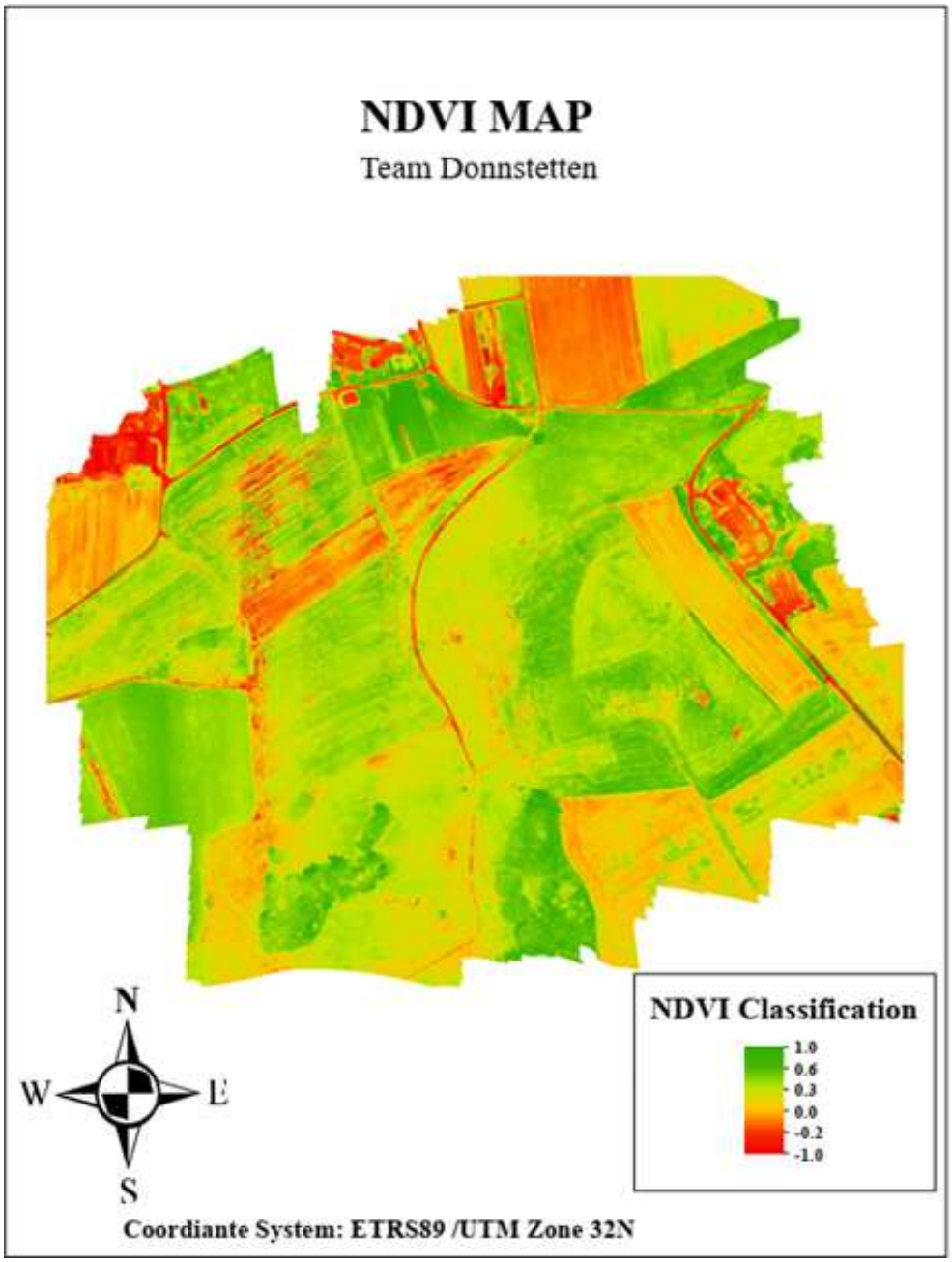

Figure 2.25: *The NDVI Map*

For the final part of the project, a comparison should be made with data from other tasks. For this purpose, the point cloud is compared with laser scanner data. The result can be seen in Figures 2.26 to 2.29.

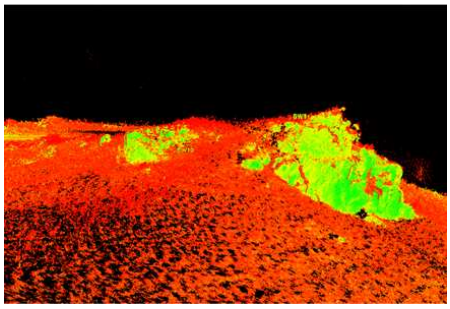

Figure 2.26: *Comparison between Drone Point Cloud and Laser scanner front view*

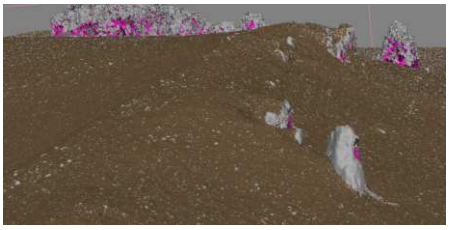

Figure 2.27: *Comparison between Drone Point Cloud and Laser scanner front view*

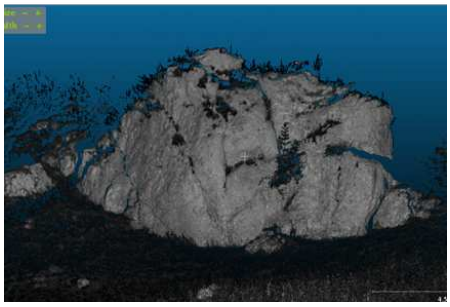

Figure 2.28: *Comparison between Drone Point Cloud and Laser scanner front view*

Figure 2.29: *Comparison between Drone Point Cloud and Laser scanner front view*

2.5 Task 5: Terrestrial Laser Scanning

Introduction

Terrestrial laser scanning (TLS) is a sophisticated technology for acquiring high-precision three-dimensional data of surfaces and structures. This technique is utilized across a wide range of applications, including archaeology, construction, forestry, and urban planning. By capturing millions of measurement points per second, TLS can generate detailed 3D models that are invaluable for both analytical and visualization purposes.
TLS operates by emitting laser beams to measure the distance to surfaces, thereby creating point clouds. These point clouds accurately and intricately represent the captured structures.

The deployment of TLS in scientific research aims to collect comprehensive topographical and structural information, which is essential for subsequent analyses and applications within the project. This data can aid in documenting and examining changes in terrain or structures, as well as in creating precise models for planning and restoration efforts.
In Figures 2.30 and 2.31, you can see the laser scanner (Leica HDS 7000), as well as the black and white (BW) targets that were specifically used for this task.

Figure 2.30: *Leica HDS 7000 laser scanner*

Figure 2.31: *Black and white targets*

In this section, the utilization of terrestrial laser scanning is elaborated, detailing the methods employed, the workflow followed, and the results obtained.

Planning Phase

During the planning phase, it was imperative to first delineate the area of interest. Once this area was defined, considerations regarding the number of required viewpoints to ensure complete coverage and adequate overlap were addressed. Additionally, black and white (BW) targets were necessary for subsequent georeferencing. For both the required free stationing and the proper positioning of these targets, ensuring good visibility and geometric arrangement was crucial. Key points to consider included:

- The number of viewpoints necessary to cover the entire area.
- The optimal placement of these viewpoints to ensure at least three fixed points are visible for free stationing.
- The placement of BW targets such that they are visible in at least two scans, while maintaining good geometry. Good geometry entails a horizontal distribution of targets across 360°.
- Ensuring visual contact between the viewpoints and the BW targets.

To facilitate preliminary planning, Google Earth was used to gain an initial impression of the survey area, allowing for the creation of a map depicting

the positions of the viewpoints and BW targets. However, during the survey, it became apparent that Google Earth's representation was not sufficiently accurate for the final planning stages. Given the complexity of our measurement area, it was necessary to generate a detailed map on-site. This required traversing the entire area of interest to accurately determine the positions. A map was subsequently created using a mobile device with location functionality, ensuring that the aforementioned points were considered. Furthermore, this mapping could only proceed after completing the fixed points from Task 2, as understanding the free stationing was dependent on them. It was also crucial to plan the equipment needed for the fieldwork, including measuring instruments, wire stands, tripods, walkie-talkies, reflectors, reflector rods, BW targets, and adapters for the BW targets.

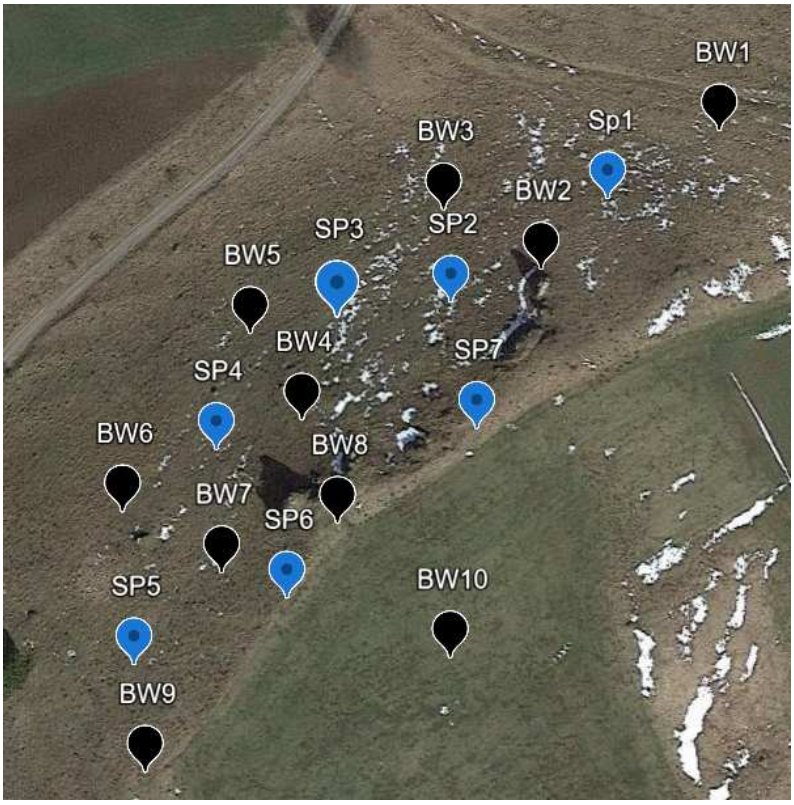

Figure 2.32: *Final plan for laser scanning*

Additionally, it was important to ensure the comparability of results with Task 4 during evaluation. Thus, the scanned area needed to overlap with the area covered by the drone flight, and at least a few BW targets from Task 4 should also be scanned in Task 5. In our case, three such targets were recorded.

Field Work

Fieldwork commenced with gathering all necessary equipment and transporting it to the survey area, ensuring that no items were forgotten and that all electronic devices, including spare batteries, were fully charged. Subsequently, a brief explanation of the work steps was provided to the team, followed by the assignment of specific tasks to individual members. Given that the tasks were not particularly complex or were familiar from previous activities, detailed explanations were unnecessary. By rotating tasks, each team member had the opportunity to perform every task at least once. The work began with the placement of reflectors over known fixed points, while the total station was set up on the first position using a tripod. Ideally, sufficient equipment, such as wire tripods, reflector rods, and reflectors, was available to simultaneously set up the fixed points and BW targets, minimizing the need for changes. Upon completion of the setup, free stationing was initiated. If the resulting accuracies were satisfactory, the individual BW targets were measured (in two faces). Proper numbering and organization of measurements were essential to prevent confusion or mix-ups during evaluation. A final check of the memory ensured that all data was correctly saved, thus avoiding the need for re-measurement. After completing the necessary measurements with the total station, it was dismantled and replaced with the laser scanner, while the tripod remained in place. Scanning was then performed, ensuring that no people or unwanted objects were present in the scan. Post-scan, the data was checked for quality and proper storage. The following points are crucial for this procedure:

- At the BW target positions, reflectors must be replaced with BW targets. If using a total station, an adapter and reflector are required, ensuring that the centers of reflectors are at the same height as the centers of BW targets. If using a laser scanner, BW targets are necessary at these points.
- Although the total station and laser scanner need not occupy the same position, doing so simplifies the process without disadvantages. It is essential, however, that the BW targets occupy consistent positions.
- The sequence of procedures is flexible; free stationing and laser scanning can occur in any order.

Once all measurements were completed, the setup was moved to the next position. This process was repeated for all viewpoints. Finally, the data from the respective devices was exported, allowing for post-processing.

Evaluation and Results

The evaluation primarily utilized the Leica Cyclone software. Initially, the center points of the BW targets were identified and labeled. Once this process was completed for each point cloud, they were merged through registration. It was critical to ensure that each BW target had the same identifier across all point clouds. The result was a unified point cloud accompanied by accuracy data.

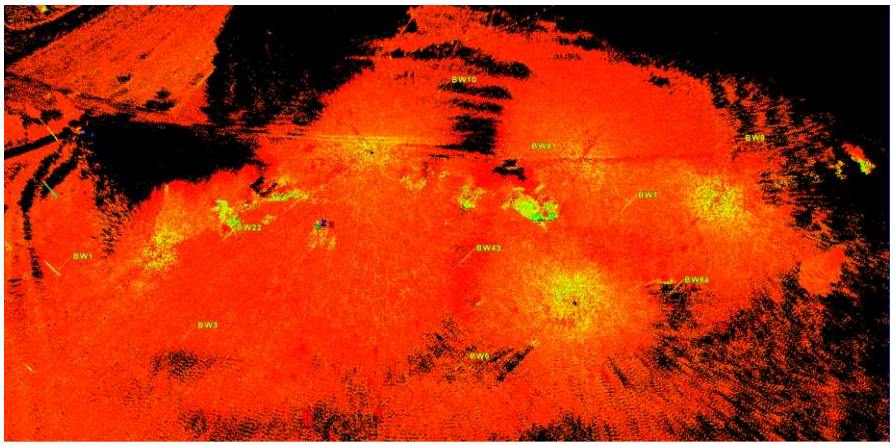

Figure 2.33: *Overview of the combined point cloud*

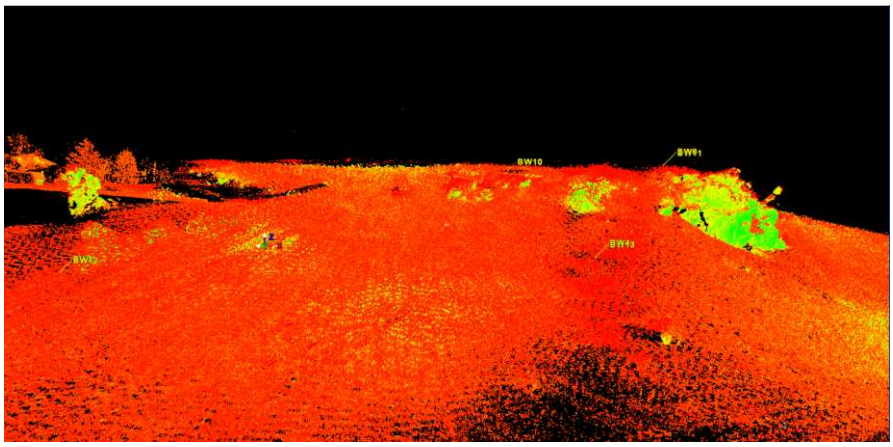

Figure 2.34: *Detailed view of a specific area*

A significant issue arose during the evaluation: the realization that at least three identical BW targets must be visible in two separate point clouds for successful registration. In four out of seven point clouds, this condition was met; however, the remaining three only had two visible targets. This issue could be partially resolved by identifying an additional common point not

corresponding to a BW target, allowing for registration but slightly reducing accuracy. The difficulty in finding identical points in natural scans, due to minor variations, was evident. As a result, reflector poles were used as the third point, though this choice negatively impacted the geometry. These factors contributed to the lower accuracy of some point clouds, as illustrated in the following table.

Table 2.21: *Accuracies with all*

Constraint ID	ScanWorld	ScanWorld	Error	Error Vector
BW3	IPD SP2	IPD SP1	0.007 m	(-0.003, -0.002, -0.006) m
BW12	IPD SP2	IPD SP1	0.010 m	(-0.009, 0.002, 0.000) m
BW5	IPD SP2	IPD SP1	0.003 m	(-0.003, -0.001, 0.000) m
BW2	IPD SP3	IPD SP1	0.007 m	(-0.003, -0.002, -0.006) m
BW4	IPD SP4	IPD SP1	0.010 m	(0.005, 0.002, 0.009) m
BW16	IPD SP6	IPD SP1	0.005 m	(-0.005, 0.004, 0.000) m
BW9	IPD SP5	IPD SP1	0.049 m	(0.003, 0.036, 0.015) m
BW8	IPD SP5	IPD SP2	0.047 m	(0.013, 0.035, 0.015) m
BW6	IPD SP5	IPD SP3	0.032 m	(0.013, 0.035, 0.015) m

Another contributing factor to the reduced accuracy was an issue with BW7. Warnings indicated either mislabeling or poor accuracy whenever this point was used. Verification confirmed correct labeling, suggesting an accuracy issue, likely due to the point being unleveled or slightly moved, resulting in errors. The accuracies for the fused point cloud without the scan from Standing point 5, which included the problematic BW7, showed improvement. The maximum error decreased from 49 mm to 22 mm, demonstrating a significant enhancement.

Table 2.22: *Accuracies without the bad BW7 in Scan 5*

Constraint ID	ScanWorld	ScanWorld	Error	Error Vector
BW3	IPD SP2	IPD SP1	0.006 m	(0.001, 0.002, -0.005) m
BW12	IPD SP2	IPD SP1	0.004 m	(0.002, -0.001, -0.003) m
BW5	IPD SP2	IPD SP1	0.013 m	(-0.003, -0.001, 0.009) m
BW2	IPD SP3	IPD SP1	0.012 m	(-0.003, -0.001, 0.001) m
BW4	IPD SP4	IPD SP1	0.006 m	(0.003, 0.001, -0.007) m
BW16	IPD SP6	IPD SP1	0.007 m	(0.003, 0.002, -0.002) m
BW9	IPD SP4	IPD SP3	0.017 m	(-0.005, -0.005, -0.011) m
BW8	IPD SP6	IPD SP3	0.012 m	(0.002, -0.004, 0.010) m
BW6	IPD SP4	IPD SP1	0.004 m	(0.004, 0.000, 0.000) m

An attempt was made to create a surface model, though the results using Leica Cyclone were suboptimal. Consequently, the software Cloud Compare was utilized, yielding much better results. Only a few places and especially a plant in the middle of the rock are shown worse, but most of it is satisfactory. In general, it can be said that it is more difficult to create a reasonable surface model when rough and uneven surfaces are present, as is usually the case in our measurement area.

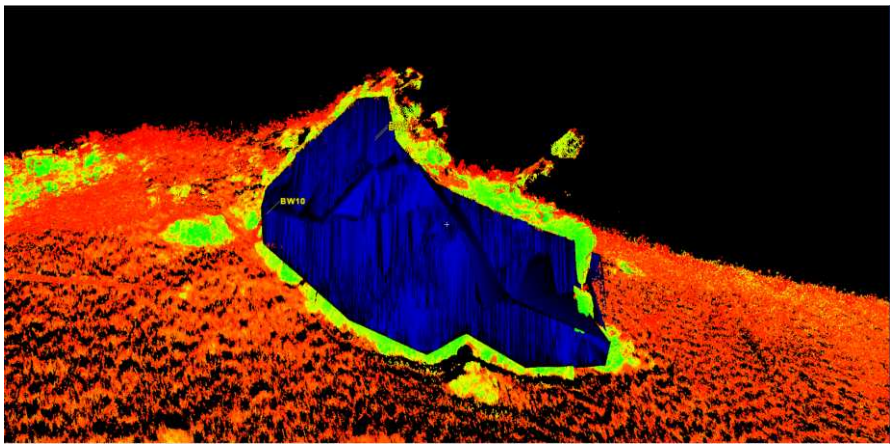

Figure 2.35: *Surface model in Leica Cyclone*

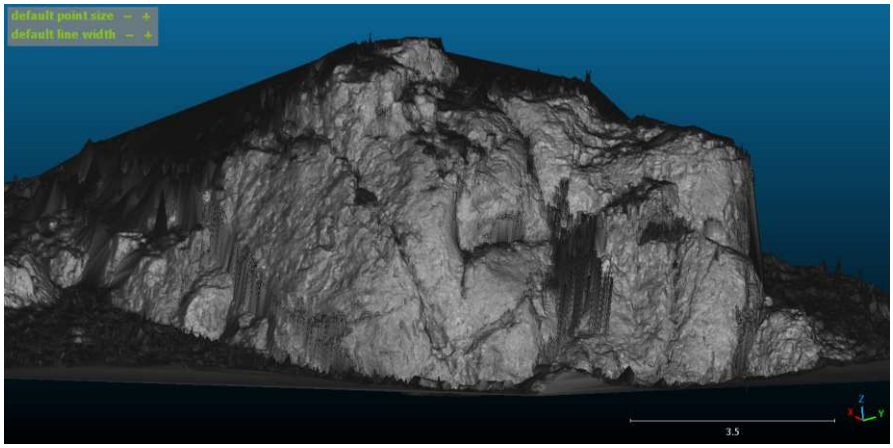

Figure 2.36: *Surface model in Cloud Compare*

2.6 Task 6: Kinematic GNSS Data Acquisition

2.6.1 Introduction

GNSS data, whether consciously or unconsciously, have become an integral part of our daily lives. Whether in airplanes, cars, or on mobile phones, they are ubiquitous and have fundamentally changed the way we navigate the world. A world without GNSS systems is now almost unimaginable. Kinematic GNSS (Global Navigation Satellite System) data acquisition is an advanced technique that enables the precise collection of position information from moving objects in real-time. This method utilizes GNSS receivers, often enhanced by real-time correction data from nearby reference stations, to continuously track and record the exact position of an object as it moves.
The Institute of Navigation Stuttgart (INS) equipped an RC car with additional hardware for measurements. Using this car and with the aid of a base station, kinematic data was collected along the terrain.

Figure 2.37: *INS RC Car*

2.6.2 Planning Phase

The measurements will be carried out using RTK (Real-Time Kinematic). For this purpose, a base station will be set up. This will be positioned at the previously known point D2 so that the data can later be compared. The base station itself connects to the satellite positioning service SAPOS to obtain even more accurate positioning data.
The final planning of the autonomous route was conducted in the field. The Area of Interest was covered, with a focus on ensuring a safe environment. By "safe," it is meant that the area is sufficiently away from slopes, free of obstacles (both on the ground and in the air), and consists of passable terrain.
The route for the manual measurements was selected to cover D1 and the elevation points on the road (FP5, FP7, FP8, and the elevation benchmark). This setup is intended to facilitate the later comparison of the positioning data with the data from other tasks.

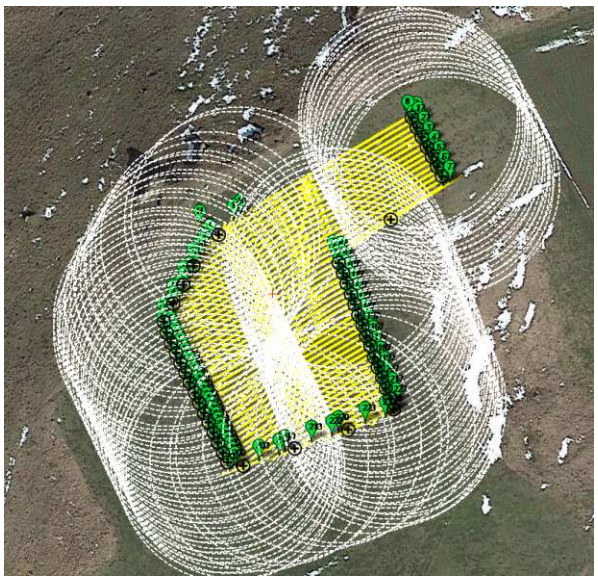

Figure 2.38: *Final Route of Autopilot*

2.6.3 Field Work

- **Base Station Setup and Device Connectivity**:
  - We began by establishing the base station in the field. All necessary devices were then connected to ensure seamless data collection throughout the operation.
- **Automated Data Collection**:
  - Using an autopilot system, we followed a predefined route plan to collect data systematically across the field area.
- **Manual Data Collection**:
  - An RC car was utilized to manually collect data at specific points of interest. This involved measuring and recording the height at each designated point.
- **Post-Processing with RTK-Lib**:
  - After completing data collection, we used RTK-Lib software for precise post-processing of the collected data to improve accuracy and reliability.
- **Data Export and Analysis**:
  - The processed data was exported, and a comprehensive point cloud was generated. This point cloud was then analyzed to extract meaningful insights and results.

Here is the map for area and positions of our points (refer to Figure 2.4).

Evaluation and Results

Route Mapping Analysis:
In this section, we present the route mapping results obtained using RTKLib software for GNSS-based tracking. RTKLib is an open-source application for precise RTK and post-processing of GNSS data, utilizing correction data from base stations and satellite services.
The images show the path taken during the operation, overlaid on different backgrounds for clarity and better understanding. Moreover, the yellow lines illustrate non-accurate areas.
The GNSS systems used for this mapping were GPS, GLONASS, and Galileo. Real-Time Kinematic (RTK) was employed to enhance the accuracy of the data. We utilized our own base station, which received correction data from the SAPOS service.

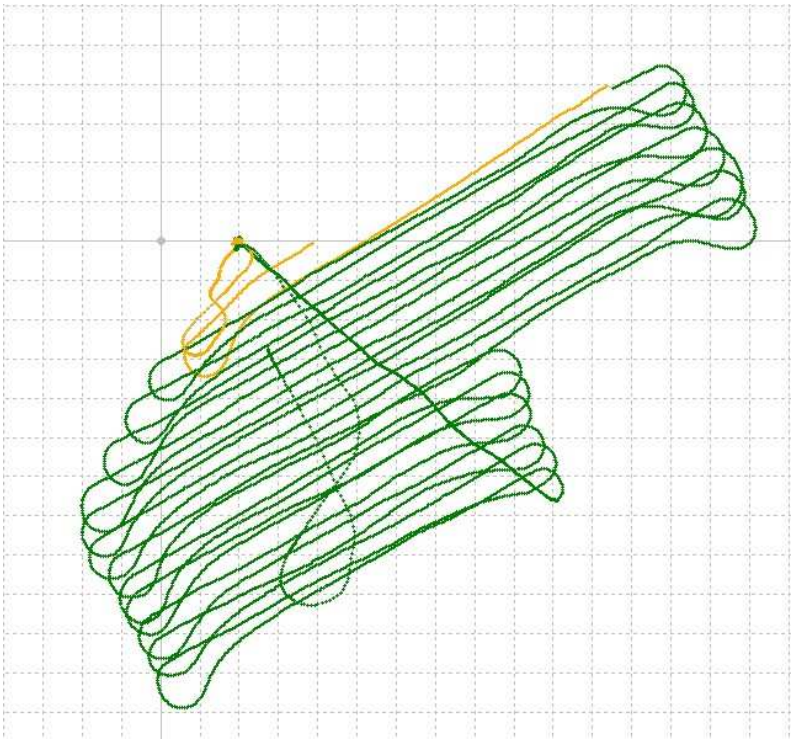

Figure 2.39: *Route overlay on a grid.*

Figure 2.40: *Route overlay on satellite imagery (closer view).*

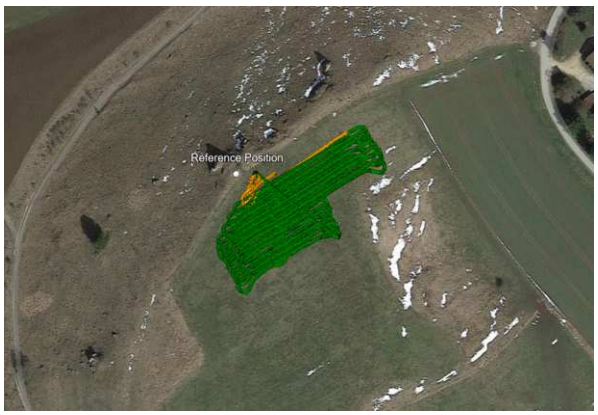

Figure 2.41: *Route overlay on satellite imagery (zoomed out view).*

The deviations from the reference coordinates indicate the precision of the GNSS measurements. The smallest deviation in the easting coordinate was observed at FP7, while the greatest deviation in height was recorded at D1. These deviations can be attributed to several factors, including signal multipath effects, atmospheric conditions, and the precision of the GNSS equipment used. Post-processing and RTK corrections were applied to minimize these errors, yet some residual discrepancies remain. These results demonstrate the high precision achieved through the kinematic GNSS data acquisition method used in this project.
These three images seem to depict the path of a GPS-tracked route overlaid on satellite maps and a grid.

1. **Figure 2.42**: This image is a plot of the GPS route from the first image displayed on a plain grid. The shape of the route is consistent with the

path seen in the first image, showing how the route was mapped out in relation to a grid.

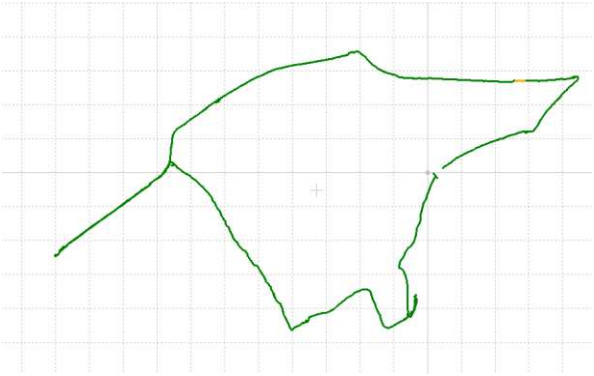

Figure 2.42: *GPS route in RTKLib*

2. **Figure 2.43**: This image also shows the GPS route on a satellite map similar to the first one, but it includes an additional segment of the route marked in yellow. This could represent a different part of the journey or an alternative path.

Figure 2.43: *GPS route with segment of the route*

The images together illustrate the comparison between GPS data plotted on a grid versus overlaid on a satellite image, showing the tracked route through the landscape.

Numerical results:

First we process our raw data in RTKlib in specific date time period Time start (GPST): 24.07.2024 at 16:35:00 and the End time (GPST): 24.07.2024 at 17:15:00 and also add the coordinate from our points and use Gallilio options to get our results. in the second step we add our RTKlib result in MATLAB code and we get some results for our points in field area.

Table 2.23: *The Numerical results*

directions	Measured coordinates(RTK)	deviation from reference
Easting	541820.487 m	-0.0158 m
Northing	5372289.059 m	0.124 m
Height	812.128 m	-1.123 m

Here is the formula that we used to achieve these results:

$$(x_1 - x_2, y_1 - y_2)$$

Table 2.24: *SAPOS Reference Coordinates*

Points	Lontitude	Latitude	Height
D1	32541820.4713	5372890.9353	813.251 m
D2	32542017.4875	5373123.0327	836.078 m

Finally we make a cloud for the height via Cloud Compare.The model exhibits a complex structure with varying heights represented by a color gradient. This color-coded elevation data suggests the model is a digital terrain model (DTM) or a digital surface model (DSM).

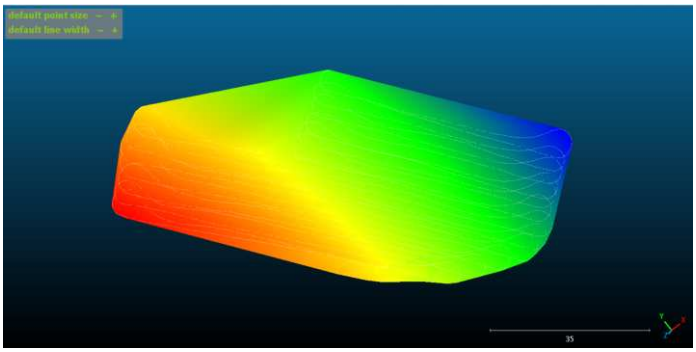

Figure 2.44: *Cloud Model of Height; blue: High, red: Low*

3

Conclusion

In summary, this year's Integrated Practicum was a success, and all planned tasks were completed to a satisfactory level, despite the many problems we faced. While some issues arose during the project, these were largely resolved or accounted for in the measurements. This enabled the creation of a control point network within the survey area, allowing for accurate geodetic mapping. Overall, we learned a great deal from this project, and our results are satisfactory. Our work provides a solid foundation for future archaeological investigations and planning in Donnstetten.

Most importantly, however, we were able to learn a great deal. Not only about the individual areas of responsibility, which errors can occur and how to rectify them, but also about the necessities for good teamwork.